# Variational radial solutions and numerical simulations for a kinetic model of a cylindrical Langmuir probe

Mehdi Badsi, Anaïs Crestetto, Ludovic Godard-Cadillac

# Variational radial solutions and numerical simulations for a kinetic model of a cylindrical Langmuir probe

M. Badsi, A. Crestetto, L. Godard-Cadillac

*Nantes Université, Laboratoire de Mathématiques Jean Leray, 2 Chemin de la Houssinière BP 92208, 44322 Nantes Cedex 3*

**Abstract**

We study, both theoretically and numerically, qualitative and quantitative properties of the solutions a Vlasov-Poisson system modeling the interaction between a plasma and a cylindrical Langmuir probe. In particular, we exhibit a class of *radial solutions* for which the electrostatic potential is increasing concave with a strong variation in the vicinity of the probe which scales as the inverse of the Debye length. These solutions are proven to exist provided the incoming distributions of particles from the plasma verify the so called *generalized Bohm condition* of plasma physics. It extends the study [1]. Small perturbations of the radial semi-Maxwellian incoming distributions are then investigated numerically. We notably observe potential barriers that lead to the existence of unpopulated trapped orbits and to the presence of particles that by bypass the probe. Curves of the collected current versus its applied voltage are also presented. This work is the continuity of the previous work [2] where the existence of solutions has been proven.

*Keywords:* cylindrical Langmuir probe; stationary Vlasov-Poisson equations; radial solutions; generalized Bohm condition; boundary layer; Debye sheath; trapped orbits;

## Introduction

The Langmuir probe is a measurement device that is used to measure the local physical properties of a plasma such as its temperature, densities and plasma potential [10, 11] known as plasma parameters. An important object of interest in the physical modeling of probes is the curve of the probe collected current versus its applied voltage. This curve is known as the probe characteristic. Usually, when the probe characteristic is known, an inverse problem depending on the assumed distribution functions of the plasma is solved to recover the plasma parameters. Questions about the variation of this curve with respect to the intrinsic physical parameters have been extensively discussed in the physics literature [4, 11, 10, 5]. Recent numerical simulations of probe characteristics using kinetic equations can be found in [5, 16, 15].

At the modeling level, it is possible to model the interaction of the probe as a stationary boundary value problem based on the Vlasov-Poisson equations [2, 1, 7, 6, 13]. The main purpose of the present work is thus to pursue our previous study [2] where we have derived the model and proven the existence of solutions. The objective is twofold: firstly, to extend the analysis notably by identifying a class of *admissible parameters* for which it is possible

to describe qualitatively and quantitatively the solutions to our model. Secondly, to do the numerical simulations of the model when the parameters are in and slightly out of the bounds of the set of *admissible parameters*.

We organized this work as follows. We begin with introducing the stationary Vlasov Poisson equations written in polar coordinates with prescribed boundary conditions. Then, we summarize the phase-space study associated with the Vlasov equations in section 2. It yields notably the reformulation of the problem as a non linear and non local Poisson problem that is presented in section 3. Due to technical obstacles, we chose to restrain the study of qualitative descriptions and quantitative estimates to a particular class of solutions for which all the particles have a null angular velocity. These solutions are called the *radial solutions* and are studied in section 4. They are obtained by minimization of an energy functional whose Euler-Lagrange equation is exactly the Poisson equation that needs to be solved. This variational approach is made possible by simplifications in the non linear source term of the Poisson equation: the non local terms vanishes. Our analysis establishes, provided the incoming distributions functions satisfy a *generalized Bohm condition*, that the electrostatic potential is monotone increasing, concave and verifies quantitative boundary layer estimates which physically pertains to the existence in the vicinity of the probe of the so-called Debye sheath [14, 4]. This study extends the one done earlier in [1]. It is more generic and the boundary layer estimates are more precise. Then, we describe in section 5 the numerical method to solve the non linear and non local Poisson problem. Namely, we introduce a fixed point approach based on a gradient descent method. In our numerical method, the electrostatic potential is approximated using a standard affine finite element approximation. The computation of the non local terms appearing in the source term of the Poisson equation are approximated using a projection on the finite element space of the quantities of interest. Space and velocity integrals are computed using standard arbitrary high order quadratures. The numerical simulation of the complete model is done in the last section. Two test cases are proposed. The first one corresponds to the numerical simulations of the *radial solutions.* We show solutions when the *generalized Bohm condition* is verified and when it is not. In both cases, a boundary layer near the probe is observed when the Debye length is small. The main difference between the two cases lies in the fact that when the *generalized Bohm condition* is not verified another boundary layer in the plasma core appears. Besides, the probe characteristics does not need to be computed for the *radial solutions* since it has an explicit expression which shows that it is independent of the Debye length, it is a monotone increasing function of the probe potential value, and it has an asymptotic value when the probe voltage becomes large. Our second test case corresponds to non *radial solutions* which are only slight perturbation of the *radial solutions*. This means that the distribution functions do carry some particles with small non zero angular velocities. This test case is prospective. We observe numerically that if the angular momentum is non zero, it is possible that some particles are trapped and do not reach the probe though the electrostatic potential is still locally near the probe monotone increasing (attractive for the ions and repulsive for the electrons). This means that a potential barrier exists for particles with not high enough energy. This observation can be interpreted as a consequence of the geometry of the trajectories of particles that bend when the angular momentum increases. We also present the curves of the probe characteristic for two different distribution functions. We still observe that it is a monotone increasing function of the probe voltage for the range

of parameters we used.

## 1. Modeling the probe

Throughout this article, we work with a collisionless plasma made of one species of ions and of electrons in which is immersed a cylindrical probe. The radius of the probe is fixed at $r_p = 1$ and the length of its axis assumed to be much bigger than 1 so that we can reduce the model to planar motion in polar coordinates centered around the probe. We work in the open set $\Omega = \{(x, y) \in \mathbb{R}^2 \ : \ 1 < \sqrt{x^2 + y^2} < r_b\}$ where $r_b$ is an outer boundary radius (see Figure 1). Outside the radius $r_b$ lays the ionizing source from which originate the particles that are in $\Omega$ the neighborhood of the probe. In other words : the radii $r > r_b$ correspond to the plasma core. We neglect the magnetic effects, and eventually, the plasma is assumed to have a rotational invariance and to be at rest so that we work only with quantities independent of the time and of the angular position.

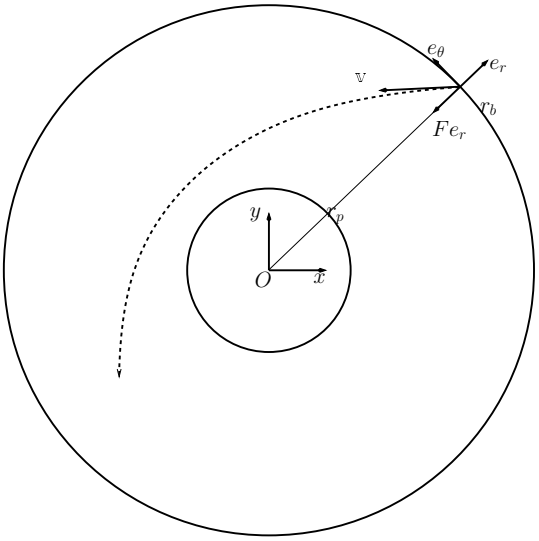


Figure 1: Sketch of a trajectory of a particle into a radial force field entering at $r = r_b$ with a velocity $\mathbb{v}$.

### *1.1. The Vlasov-Poisson equations in polar coordinates*

The unknown of the problem are the two particles distribution respectively for the ions and for the electrons, noted respectively $f_i$ and $f_e$ and the macroscopic electrostatic potential $\phi$. Given the symmetries and invariants of the problem, the particles distributions depend only on the radius $r \in [1, r_b]$, on the radial velocity $v_r$ and on the angular velocity $v_\theta$. Similarly, the electrostatic potential $\phi$ depends only on the radial variable. Writing now the Vlasov-Poisson equation in polar coordinates, we obtain the system of dimensionless

equations studied in this article:

$$v_r\,\partial_r f_i - \frac{v_r v_\theta}{r}\partial_{v_\theta} f_i + \left(\frac{v_\theta^2}{r} - \partial_r\phi\right)\partial_{v_r} f_i = 0, \qquad \forall (r, v_r, v_\theta) \in (1, r_b)\times\mathbb{R}^2 \tag{1}$$

$$v_r\,\partial_r f_e - \frac{v_r v_\theta}{r}\partial_{v_\theta} f_e + \left(\frac{v_\theta^2}{r} + \partial_r\phi\right)\partial_{v_r} f_e = 0, \qquad \forall (r, v_r, v_\theta) \in (1, r_b)\times\mathbb{R}^2 \tag{2}$$

$$-\frac{\lambda^2}{r}\frac{d}{dr}\left(r\frac{d\phi}{dr}\right)(r) = n_i(r) - n_e(r), \qquad \forall r \in (1, r_b), \tag{3}$$

where $n_i$ and $n_e$ are macroscopic charge densities respectively of the ions and of the electrons:

$$n_i(r) := \int_{\mathbb{R}^2} f_i(r, v_r, v_\theta)\, dv_r\, dv_\theta, \quad n_e(r) := \int_{\mathbb{R}^2} f_e(r, v_r, v_\theta)\, dv_r\, dv_\theta. \tag{4}$$

The physical parameter $\lambda > 0$ is a normalized Debye length. These four equations (1)-(4) will be referred throughout this article as the "Stationary Radial 2-species Vlasov-Poisson equation", that we shortly denote (SR2VP). We also define for $r \in [1, r_b]$ the radial ionic and electronic current density (which difference at $r = 1$ is the quantity measured by the experimenter):

$$j_i(r) := \int_{\mathbb{R}^2} f_i(r, v_r, v_\theta)\, v_r\, dv_r\, dv_\theta, \qquad j_e(r) := \frac{1}{\sqrt{\mu}}\int_{\mathbb{R}^2} f_e(r, v_r, v_\theta)\, v_r\, dv_r\, dv_\theta, \tag{5}$$

where $\mu > 0$ is the mass ratio between an ion and an electron. Concerning the boundary conditions at $r = r_b$, the ionizing source outside is modeled by a distribution of incoming ions $f_i^b$ and of incoming electrons $f_e^b$. The origin of the potentials is chosen to be in the plasma core. For the boundary condition at $r = 1$, the probe is assumed to be non-emitting of particles and the potential at the probe is fixed by the experimenter to some given value $\phi_p$. In short:

$$f_i(r_b, v_r, v_\theta) = f_i^b(v_r, v_\theta), \quad f_e(r_b, v_r, v_\theta) = f_e^b(v_r, v_\theta), \quad \forall (v_r, v_\theta) \in \mathbb{R}_-^* \times \mathbb{R}, \tag{6}$$

$$f_i(1, v_r, v_\theta) = 0, \quad f_e(1, v_r, v_\theta) = 0, \quad \forall (v_r, v_\theta) \in \mathbb{R}_*^+ \times \mathbb{R} \tag{7}$$

$$\phi(1) = \phi_p, \quad \phi(r_b) = 0. \tag{8}$$

## 2. Phase space study for the Vlasov equations

We now briefly recall the methodology used in [2] to study the Vlasov equations. For a more extensive presentation and the proofs, we refer to this paper. The first step consists in fixing the electrostatic potential $\phi$ to be any function in $W^{2,\infty}[1, r_b]$ that satisfies the Dirichlet boundary conditions $\phi(1) = \phi_p$, $\phi(r_b) = 0$. Then, we solve explicitely the Vlasov equations with the method of characteristics. To obtain explicit formulas, we heavily rely on the invariants and symmetries of the problem. The equations of the characteristics both for the ionic and electronic phase diagram shows two conserved quantities. These are respectively the total energy and the angular momentum:

$$e := \frac{{v_r}^2}{2} + \frac{{v_\theta}^2}{2} \pm \phi(r), \qquad \text{and} \qquad L := r\, v_\theta.$$

The physical convention is that for the ions the total energy corresponds to the potential $+\phi$ while for the electrons it corresponds to its opposite $-\phi$. For a given fixed angular momentum $L \in \mathbb{R}$, it is natural to introduce the effective potential $\mathcal{U}_L$ which is defined for any continuous function $\psi : [1, r_b] \to \mathbb{R}$ by

$$\begin{array}{rccc} \mathcal{U}_L[\psi] : & [1, r_b] & \to & \mathbb{R} \\ & r & \mapsto & \psi(r) + L^2/(2r^2). \end{array} \tag{9}$$

In particular, taking $\psi = \phi$ corresponds to the ionic effective potential while taking $\psi = -\phi$ corresponds to the electronic one. The effective potential allows us to reduce the analysis of the particles trajectories to the radial dynamics. Indeed, the conservation of the total energy and the angular momentum may be equivalently re-written as

$$e := \frac{{v_r}^2}{2} + \mathcal{U}_L[\pm\phi](r), \qquad \text{and} \qquad L := r\, v_\theta.$$

So, for each given value of the angular momentum $L \in \mathbb{R}$, the phase space $(r, v_r)$ may be decomposed as the union of level (of energy) curves of the function $(r, v_r) \mapsto \frac{{v_r}^2}{2} + \mathcal{U}_L[\pm\phi](r)$. Then, the trajectories are separated into two categories, depending on whether their energy is higher or lower than the maximum value of the effective potential which is a potential barrier. In this regard, we introduce the effective potential barrier also called *max-parameter*: it is defined for any continuous function $\psi : [1, r_b] \to \mathbb{R}$ by

$$\overline{\mathcal{U}_L}[\psi] := \max_{r \in [1, r_b]} \mathcal{U}_L[\psi](r). \tag{10}$$

To get rid of closed curves in the phase diagram (supposed empty of particles in the permanent regime), we need to introduce the *barrier-parameter*: it is defined for any continuous function $\psi : [1, r_b] \to \mathbb{R}$ by

$$\widetilde{\rho}[\psi] := \min\left\{a \in [1, r_b] \ : \ \text{for all}\, s \in [a, r_b],\ \psi(s) \le 0\right\}. \tag{11}$$

Then for each $(L, e) \in \mathbb{R}^2$, the lowest radius reached by the particles of energy $e$ and angular momentum $L$ coming from the plasma core associated with an abstract potential function $\psi : [1, r_b] \longrightarrow \mathbb{R}$ is defined by

$$r[\psi](L, e) := \widetilde{\rho}\left[\mathcal{U}_L[\psi] - e\right]. \tag{12}$$

An example of possible phase diagram for radial dynamics associated with an abstract potential $\psi$ is drawn at Figure 2. This eventually leads to the decomposition of the phase space $(r, v_r)$ between characteristics that have high energy and characteristics that have low energy (for a fixed value of $L$):

$$\mathcal{D}^b[\psi](L) := \mathcal{D}^{b,1}[\psi](L) \cup \mathcal{D}^{b,2}[\psi](L), \tag{13}$$

$$\mathcal{D}^{b,1}[\psi](L) = \left\{(r, v_r) \in (1, r_b) \times \mathbb{R} \ : \ v_r < -\sqrt{2\left(\overline{\mathcal{U}_L}[\psi] - \mathcal{U}_L[\psi](r)\right)}\right\}, \tag{14}$$

$$\mathcal{D}^{b,2}[\psi](L) = \left\{(r, v_r) \in (1, r_b) \times \mathbb{R} \ : \mathcal{U}_L[\psi](r_b) < \underbrace{\frac{v_r^2}{2} + \mathcal{U}_L[\psi](r)}_{=:e} < \overline{\mathcal{U}_L}[\psi]\ ,\ r > r[\psi](L, e)\right\}. \tag{15}$$

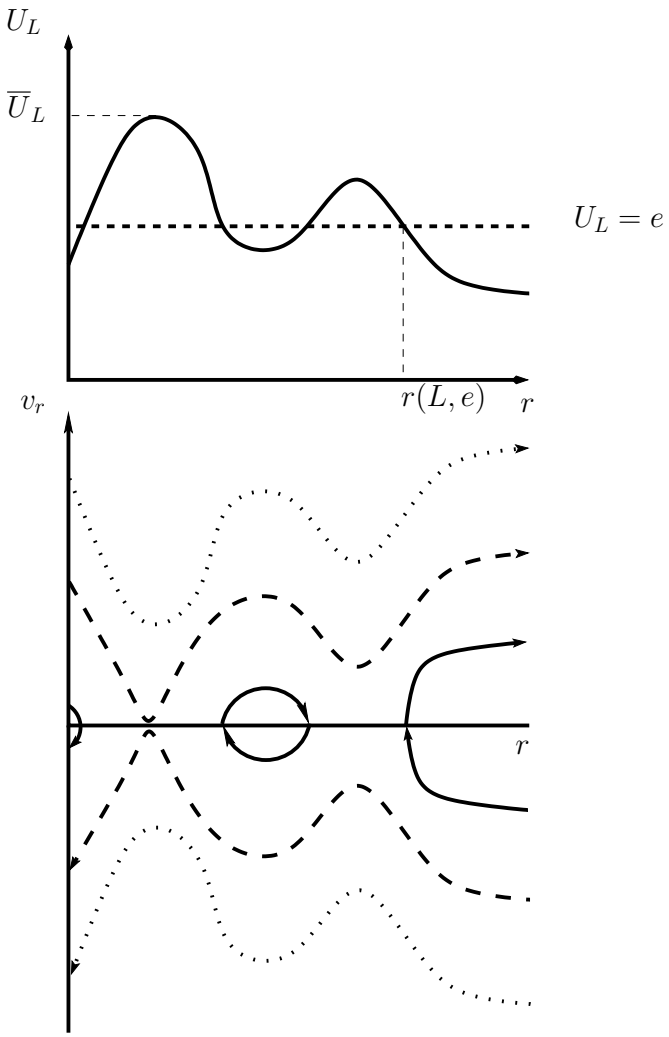


Figure 2: Schematic $(r, v_r)$ phase space decomposition corresponding to an effective potential $\mathcal{U}_L[\psi]$ for some $\psi$. Dotted lines correspond to trajectories of energy level greater than $\overline{\mathcal{U}_L}[\psi]$. The dashed line corresponds to a separatrix curve of equation $\frac{v_r^2}{2} + \mathcal{U}_L[\psi](r) = \overline{\mathcal{U}_L}[\psi]$. The solid lines correspond to trajectories of energy level lower than $\overline{\mathcal{U}_L}[\psi]$.

Using this generic phase space decomposition, we construct explicitly a solution to the Vlasov equation. For the sake of conciseness, we shall often use the subscript $\alpha \in \{i, e\}$ to denote a quantity that corresponds to the ions when $\alpha = i$ or to the electrons when $\alpha = e$. We therefore obtain expressions for weak solution of Vlasov equation, as detailed in the two following propositions obtained at [2].

**Proposition 2.1** (Weak solution for the Vlasov equation)**.** *Let $\alpha \in \{i, e\}$. Set $\psi = \phi$ if $\alpha = i$ or $\psi = -\phi$ if $\alpha = e$. Let $L \in \mathbb{R}$, then for each point $(r, v_r) \in \mathcal{D}^b[\psi](L)$ defined above there exists a unique characteristics curve that passes through $(r, v_r)$ and originates from $r = r_b$ with a negative velocity $v_b = -\sqrt{v_r^2 + 2(\mathcal{U}_L[\psi](r) - \mathcal{U}_L[\psi](r_b))}$. Moreover, a weak solution of*

*the Vlasov equation for the species $\alpha$ is given by:*

$$f_\alpha(r,v_r,v_\theta) := \begin{cases} f_\alpha^b\left(-\sqrt{v_r^2+2(\mathcal{U}_L[\psi](r)-\mathcal{U}_L[\psi](r_b))};\frac{rv_\theta}{r_b}\right) & \text{if } (r,v_r)\in\mathcal{D}^b[\psi](L) \text{ with } L=rv_\theta,\\ 0 \quad \text{otherwise.}\end{cases} \tag{16}$$

Using this explicit construction, we express the macroscopic density and current explicitly in terms of the effective potential $\mathcal{U}_L[\psi]$.

**Proposition 2.2.** *Let $\alpha\in\{i,e\}$. Set $\psi=\phi$ if $\alpha=i$ or $\psi=-\phi$ if $\alpha=e$. Consider $f_\alpha^b : \mathbb{R}_-^*\times\mathbb{R}\to\mathbb{R}^+$ a distribution of velocities for incoming charged particles which is moreover symmetric with respect to the angular velocity variable. With $f_\alpha$ defined by* (16) *the macroscopic density is given by*

$$\begin{aligned} rn_\alpha(r) &= 2\int_0^{+\infty}\int_{-\infty}^{-\sqrt{2(\overline{\mathcal{U}_L}[\psi]-\mathcal{U}_L[\psi](r_b))}} \frac{|w|}{\sqrt{w^2-2(\mathcal{U}_L[\psi](r)-\mathcal{U}_L[\psi](r_b))}} f_i^b\left(w,\frac{L}{r_b}\right)\,dw\,dL\\ &+4\int_0^{+\infty}\int_{\mathcal{W}_\alpha(r,L)} \frac{|w|}{\sqrt{w^2-2(\mathcal{U}_L[\psi](r)-\mathcal{U}_L[\psi](r_b))}} f_i^b\left(w;\frac{L}{r_b}\right)\,dw\,dL \end{aligned} \tag{17}$$

*where*

$$\mathcal{W}_\alpha(r,L) := \Big\{ w\in\mathbb{R} \,:\, -\sqrt{2(\overline{\mathcal{U}_L}[\psi]-\mathcal{U}_L[\psi](r_b))} < w < -\sqrt{2(\mathcal{U}_L[\psi](r)-\mathcal{U}_L[\psi](r_b))_+} \quad \text{and} \quad r>r[\psi]\left(L,\frac{w^2}{2}+\mathcal{U}_L[\psi](r_b)\right)\Big\}.$$

*The radial current density is given by:*

$$j_\alpha(r)=\frac{2}{r}\int_0^{+\infty}\int_{-\infty}^{-\sqrt{2(\overline{\mathcal{U}_L}[\psi]]-\mathcal{U}_L[\psi](r_b))}} f_\alpha^b\left(w;\frac{L}{r_b}\right)\,w\,dw\,dL. \tag{18}$$

We recall the definition of the positive part of a number $x\in\mathbb{R}$ which is $(x)_+ := \max\{x,0\}$ and the negative part $(x)_- := \max\{-x,0\}$. Eventually, to have a formulation that is shorter and easier to manipulate, we introduce the function:

$$\begin{array}{rccl} \Gamma: & \mathbb{R}\times[1,r_b]\times\mathbb{R}\times\mathbb{R} & \longrightarrow & \mathbb{R}\\ & (\nu,r,w,L) & \longmapsto & \begin{cases} \dfrac{(w)_-}{\sqrt{w^2-2\nu+L^2\left(\frac{1}{r^2}-\frac{1}{r_b^2}\right)}} & \text{if } w^2>2\nu+L^2\left(\frac{1}{r^2}-\frac{1}{r_b^2}\right),\\ 0 & \text{otherwise.}\end{cases}\end{array} \tag{19}$$

We can rewrite the formulation of $rn_\alpha$ for $\alpha\in\{i,e\}$ in a more compact way as follows (see [2] for details):

$$rn_\alpha(r)=\int_{\mathbb{R}^2}\Gamma\big(\psi(r),r,w,L\big)\,f_\alpha^b\left(w,\frac{L}{r_b}\right)\left(1+\mathbb{1}_{w^2+\frac{L^2}{r_b^2}<2\overline{\mathcal{U}_L}[\psi]}\right)\mathbb{1}_{r\geq r[\psi]\left(L,\frac{w^2}{2}+\frac{L^2}{2r_b}\right)}\,dw\,dL, \tag{20}$$

where $\psi=\phi$ if $\alpha=i$ and $\psi=-\phi$ if $\alpha=e$.

## 3. Reformulation as a non-linear and non-local Poisson problem

The analysis of existence of solutions in [2] relies on a reformulation of the full problem into a non-linear and non-local Poisson equation. The first step is to reformulate the non linear term (20) so as to make explicit the dependency on the non local terms. In this regard, we see in the formula (20) that the non local terms are the *max-parameter* given by (10) and the *barrier-parameter* given by (12). They are non local because for a given continuous function $\psi : [1, r_b] \longrightarrow \mathbb{R}$ the computation for each $(L, e) \in \mathbb{R}^2$ of $\overline{\mathcal{U}_L}[\psi]$ and $\widetilde{\rho}\,[\mathcal{U}_L[\psi] - e]$ requires the values of $\psi$ on the whole interval $[1, r_b]$. We then define the non linear term in the Poisson equation (3) as a functional, which to any continuous function $\psi : [1, r_b] \to \mathbb{R}$ associates with another function defined for all $(\nu, r) \in \mathbb{R} \times [1, r_b]$ by

$$n[\psi](\nu, r) = g_i[\psi](\nu, r) - g_e[-\psi](-\nu, r), \tag{21}$$

where for $\alpha \in \{i, e\}$ and for any continuous function $\psi : [1, r_b] \to \mathbb{R}$ the function $g_\alpha[\psi] : \mathbb{R} \times [1, r_b] \to \mathbb{R}$ is given for all $(\nu, r) \in \mathbb{R} \times [1, r_b]$ by

$$g_\alpha[\psi](\nu, r) = \int_{\mathbb{R}^2} \Gamma\big(\nu, r, w, L\big)\, f_\alpha^b\left(w, \frac{L}{r_b}\right)\left(1 + \mathbb{1}_{w^2 + \frac{L^2}{r_b^2} < 2\overline{\mathcal{U}_L}[\psi]}\right) \mathbb{1}_{r \geq \widetilde{\rho}\left[\psi + \frac{L^2}{2}\left(\frac{1}{\bullet^2} - \frac{1}{r_b^2}\right) - w^2\right]}\, dw\, dL, \tag{22}$$

where the notation $\bullet$ is a shortcut for the identity function on $[1, r_b]$ (for the radial variable). With this definition, one sees that for all $r \in [1, r_b]$, $r n_i(r) = g_i[\phi](\phi(r), r)$ and $r n_e(r) = g_e[-\phi](-\phi(r), r)$. Therefore the Poisson equation (3) reformulates as

$$-\lambda^2 \frac{d}{dr}\left(r \frac{d\phi}{dr}\right)(r) = n[\phi](\phi(r), r), \quad r \in (1, r_b), \tag{23}$$

where the non linear source term is now given by (21). We see in the source term of the Poisson equation (23), that the local part corresponds to the the evaluation at $(\phi(r), r)$, while the non local part is encoded in the bracket $[\phi]$. In [2], we proved the following theorem.

**Theorem 3.1** (Existence of solutions for (SR2VP))**.** *Let $\phi_p \in \mathbb{R}$. Let $f_i^b$ and $f_e^b$ be two non-negative integrable functions defined on $\mathbb{R}_- \times \mathbb{R}$ symmetrical for the angular velocity variable. Assume moreover that, for $\alpha \in \{i, e\}$,*

$$\int_{\mathbb{R}} \sup_{w \in \mathbb{R}} \left| w\, f_\alpha^b(w, L) \right| dL < +\infty \qquad \text{and} \qquad \int_{\mathbb{R}} \sup_{L \in \mathbb{R}} \left| f_\alpha^b(w, L) \right| \frac{dw}{|w|^\gamma} < +\infty$$

*for some $0 < \gamma < 1$.*

*Then the stationary radial 2-species Vlasov-Poisson equations* (1)(2)(3)(4) *with boundary values $f_i^b$, $f_e^b$ and $\phi_p$ as in* (6)(7)(8) *admits a solution (a weak solution for the Vlasov equation and strong solution for the Poisson equation). Moreover, a solution to the Vlasov equation is explicitly given by* (16) *and $\phi$ is a solution to the non linear and non local Poisson equation* (23)*.*

## 4. Variational radial solutions

In this section, we are interested in the description of the solutions when the particles move radially both qualitatively and quantitatively as $\lambda \longrightarrow 0$. It is already known [4, 3, 14] that when particles move only in one direction, the plasma usually forms in a vicinity of the metallic surface a positively charged boundary layer of several Debye length in thickness called the sheath. This phenomena is caused by the relative difference of mobility between electrons and ions. Indeed, the thermal velocity of the electrons being by several order of magnitude greater than that of the ions, electrons are prone to exit the core plasma to the metallic surface at a higher rate than the ions. As a consequence, the metallic surface charges negatively and leaves the neighbouring plasma with a net positive charge. As this phenomenon alone would result in a growing positive charge in the core plasma, a mechanism of regulation settles. Namely, the accumulated negative charge at the metallic surface causes a potential drop between the core plasma and the metallic surface and produces an electric field which accelerates the ions and decelerate the electrons. The magnitude of the drop is such that an equal number (per unit of time) of positive and negative charges reach the metallic surface. When the Debye length $\lambda$ becomes small, the plasma is expected to be quasi-neutral in the sense that the size of the sheath becomes comparatively small while the core plasma stays neutral. At the mathematical level, the limit $\lambda \longrightarrow 0$ when a boundary layer is formed has already been justified rigorously in [1, 8]. Nevertheless, in [1], only a convergence to zero in the weak $H^{-1}$-norm for the macroscopic density has been proven. Here, we shall establish stronger quantitative estimates showing that the potential converges locally uniformly to zero and strongly to zero for the $L^2$-norm. As a by-product of these estimates, we obtain the convergence to zero in $L^1$-norm of the macroscopic density $r(n_i - n_e)$.

For now, we consider a particular class of incoming boundary distribution functions for $\alpha \in \{i, e\}$ of the form

$$f_\alpha^b(v_r, v_\theta) = g_\alpha^b(v_r) \otimes \delta_{v_\theta = 0}, \tag{24}$$

where $g_\alpha^b : \mathbb{R}_-^* \to \mathbb{R}^+$ is an arbitrary incoming distribution function in the radial velocity variable. Formally, the solutions for the Vlasov equation may be written as

$$f_\alpha(r, v_r, v_\theta) = g_\alpha(r, v_r) \otimes \delta_{v_\theta = 0}, \tag{25}$$

where the function $g_\alpha$ is given by

$$g_\alpha(r, v_r) = \begin{cases} g_\alpha^b\left(-\sqrt{v_r^2 + 2(\mathcal{U}_0[\psi](r) - \mathcal{U}_0[\psi](r_b))}\right) \text{ if } (r, v_r) \in \mathcal{D}^b[\psi](0), \\ 0 \quad \text{otherwise,} \end{cases} \tag{26}$$

where we recall that the potential is such that $\psi = \phi$ if $\alpha = i$ and $\psi = -\phi$ if $\alpha = e$. This formal solution will be made rigorous here after.

### *4.1. Continuity of the non linear term*

To justify rigorously the formal solution (25), we must justify the use of mono-kinetic incoming distribution functions of the form (24) in the non linear source term (21) which a priori integrates $L^1_{\text{loc}}$ functions with respect to the Lebesgue measure $\mathrm{d}w \otimes \mathrm{d}L$. We therefore begin to prove the continuity of the partial integral with respect to $L$ so that it is legitimate to integrate with respect to the Dirac measure in the angular variable $\mathrm{d}w \otimes \delta_{L=0}\mathrm{d}L$. One has the following.

**Proposition 4.1** (Continuity property for the partial integrals defining $rn_\alpha$)**.** *Let $\phi$ be a $W^{2,\infty}[1,r_b]$ function. Let $\alpha \in \{i,e\}$. Set $\psi = \phi$ if $\alpha = i$ or $\psi = -\phi$ if $\alpha = e$. Define $\Gamma$ with (19), $\overline{\mathcal{U}_L}[\psi]$ with (9)-(10) and $r[\psi](L,e)$ by (12). Assume that the boundary datum $f^b_\alpha$ is of the form (24) where $g^b_\alpha$ verifies*

$$\sup_{w\in\mathbb{R}} \left| w\, g^b_\alpha(w) \right| < +\infty, \qquad \text{and} \qquad \int_{\mathbb{R}} g^b_\alpha(w)\, dw < +\infty. \tag{27}$$

*Then for each $r \in [1,r_b]$, the following function:*

$$L \;\longmapsto\; \int_{\mathbb{R}} \Gamma\big(\psi(r),r,w,L\big)\, g^b_\alpha(w) \left(1 + \mathbb{1}_{w^2+\frac{L^2}{r_b^2} < 2\overline{\mathcal{U}_L}}\right) \mathbb{1}_{r\geq r[\psi](L,w^2/2+L^2/2r_b)}\, dw \tag{28}$$

*is continuous on $\mathbb{R}$.*

*Proof.* First, it is a consequence of the topological properties for $r[\psi](L,e)$ established at [2] (Proposition 5.7) that the function $L \mapsto r[\psi]\,(L, w^2/2 + L^2/2r_b)$ is continuous for almost every $w$. It is also direct to check that $L \mapsto \overline{\mathcal{U}_L}[\psi]$ is continuous since the operator *max* preserves the continuity property. We conclude that

$$L \;\longmapsto\; \Gamma\big(\psi(r),r,w,L\big)\, g^b_\alpha(w) \left(1 + \mathbb{1}_{w^2+\frac{L^2}{r_b^2} < 2\overline{U_L}}\right) \mathbb{1}_{r\geq r[\psi](L,w^2/2+L^2/2r_b)}$$

is continuous for almost every $w$.

We now study the function defined at (28). From the definition of $\Gamma$ we see that if $L_n$ is a sequence converging towards some fixed $L \in \mathbb{R}$, then for $n$ large enough:

$$\left|\Gamma\big(\nu,r,w,L_n\big)\right| \;\leq\; 2\frac{|w|}{\left|w^2 - L^2\left(\frac{1}{r^2} - \frac{1}{{r_b}^2}\right) - 2\nu\right|^{\frac{1}{2}}}. \tag{29}$$

To obtain the announced continuity property using the Lebesgue dominated convergence theorem, there remain to obtain the integrability property. The proof is reminiscent from Lemma 5.1 in [2]. Let $L,\nu \in \mathbb{R}$ and let $r \in [1,r_b]$. We define the set

$$\mathcal{O}_r^{L,\nu} := \left\{ w \in \mathbb{R} : \left| w^2 - L^2\left(\frac{1}{r^2} - \frac{1}{r_b^2}\right) - 2\nu \right| \;\leq\; \frac{w^2}{2} \right\}.$$

By definition of $\mathcal{O}_r^{L,\nu}$,

$$\int_{\mathbb{R}\setminus\mathcal{O}_r^{L,\nu}} \frac{|w|}{\left|w^2 - L^2\left(\frac{1}{r^2} - \frac{1}{r_b^2}\right) - 2\nu\right|^{\frac{1}{2}}} \left|g^b_\alpha(w)\right| dw \;\leq\; \sqrt{2}\int_{\mathbb{R}} g^b_\alpha(w)\, dw. \tag{30}$$

On the other hand,

$$\begin{aligned} w \in \mathcal{O}_r^{L,\nu} \quad &\Longleftrightarrow \quad -\frac{1}{2}w^2 \leq L^2\left(\frac{1}{r^2} - \frac{1}{r_b^2}\right) + 2\nu \leq \frac{3}{2}w^2 \\ &\Longleftrightarrow \quad \frac{L^2\left(\frac{1}{r^2} - \frac{1}{r_b^2}\right) + 2\nu}{3/2} \leq w^2 \leq \frac{L^2\left(\frac{1}{r^2} - \frac{1}{r_b^2}\right) + 2\nu}{1/2}. \end{aligned} \tag{31}$$

We see that, for $\lambda$ a positive number,

$$\begin{aligned}\int_{\frac{\lambda}{\sqrt{3/2}}}^{\lambda} \frac{dw}{\left|w^2-\lambda^2\right|^{\frac{1}{2}}} &\leq \int_{\frac{\lambda}{\sqrt{3/2}}}^{\lambda} \frac{dw}{\left|(\lambda+w)(\lambda-w)\right|^{\frac{1}{2}}} \leq \frac{1}{\left|\lambda+\frac{\lambda}{\sqrt{3/2}}\right|^{\frac{1}{2}}} \int_{\frac{\lambda}{\sqrt{3/2}}}^{\lambda} \frac{dw}{\left|\lambda-w\right|^{\frac{1}{2}}} \\ &= 2\frac{\left|1-\frac{1}{\sqrt{3/2}}\right|^{\frac{1}{2}}}{\left|1+\frac{1}{\sqrt{3/2}}\right|^{\frac{1}{2}}} \leq 2.\end{aligned} \tag{32}$$

Similarly,

$$\int_{\lambda}^{2\lambda} \frac{dw}{\left|w^2-\lambda^2\right|^{\frac{1}{2}}} \leq 2. \tag{33}$$

We note that (31) implies that $\mathcal{O}_r^{L,\nu}$ is non-empty if and only if $L^2(1/r^2-1/r_b^2)+2\nu \geq 0$. In this case we can choose $\lambda$ such that $\lambda^2 = L^2(1/r^2-1/r_b^2)+2\nu$. Then the computations (32) and (33) imply

$$\begin{aligned}&\int_{\mathcal{O}_r^{L,\nu}} \frac{|w| f(w,L)}{\left|w^2-L^2\left(\frac{1}{r^2}-\frac{1}{r_b^2}\right)-2\nu\right|^{\frac{1}{2}}}\, dw \\ \leq\ & \Big(\sup_w |w|\, g_\alpha^b(w)\Big) \int_{\mathcal{O}_r^{L,\nu}} \frac{1}{\left|w^2-L^2\left(\frac{1}{r^2}-\frac{1}{r_b^2}\right)-2\nu\right|^{\frac{p}{2}}}\, dw \\ \leq\ & 4\Big(\sup_w |w|\, g_\alpha^b(w)\Big).\end{aligned} \tag{34}$$

If we now gather (30) and (34):

$$\int_{-\infty}^{+\infty} \frac{|w|\, g_\alpha^b(w)}{\left|w^2-L^2\left(\frac{1}{r^2}-\frac{1}{r_b^2}\right)-2\nu\right|^{\frac{1}{2}}}\, dw \leq \sqrt{2}\int_{\mathbb{R}} g_\alpha^b(w)\, dw + 4\Big(\sup_w |w|\, g_\alpha^b(w)\Big).$$

We conclude to the integrability property using the hypothesis (27). So the Lebesgue dominated convergence theorem applies and the claim is proved. □

Owing to this continuity property, we then obtain the following.

**Corollary 4.2** (Reduction)**.** *Let $\phi_p < 0$. Let $\phi \in W^{2,\infty}[1,r_b]$. Assume $\phi$ is increasing on $[1,r_b]$ with $\phi(1)=\phi_p$ and $\phi(r_b)=0$. Consider for $\alpha \in \{i,e\}$, the boundary data $f_\alpha^b$ of the form* (24) *and satisfying the assumption of Proposition 4.1. Then, the macroscopic densities reduce for all $r \in [1,r_b]$ to*

$$rn_i(r) = \int_{-\infty}^{0} \frac{|w|}{\sqrt{w^2-2\phi(r)}} g_i^b(w)\, dw, \tag{35}$$

$$rn_e(r) = \int_{-\infty}^{\sqrt{2(\phi(r)-\phi_p)}} g_e^b\left(-\sqrt{v^2-2\phi(r)}\right) dv. \tag{36}$$

*If in addition*

$$\int_{\mathbb{R}_-} g_\alpha^b(w)|w|dw < +\infty, \tag{37}$$

*then the current densities reduce to*

$$j_i(r) = \frac{1}{r}\int_{-\infty}^{0} g_i^b(w) w\, dw, \tag{38}$$

$$j_e(r) = \frac{1}{r\sqrt{\mu}}\int_{-\infty}^{-\sqrt{-2\phi_p}} g_e^b(w) w dw. \tag{39}$$

*Proof.* Set $\psi = \phi$ if $\alpha = i$ or $\psi = -\phi$ if $\alpha = e$. Using the Proposition 4.1, for $r \in [1, r_b]$ the function

$$L \longmapsto \int_{\mathbb{R}} \Gamma\big(\psi(r), r, w, L\big)\, g_\alpha^b(w)\left(1 + \mathbb{1}_{w^2 + \frac{L^2}{r_b^2} < 2\overline{U_L}}\right)\mathbb{1}_{r \geq r[\psi](L, w^2/2 + L^2/2r_b)}\, dw$$

is continuous. Then integrating with respect to the Dirac measure $\delta_{L=0}dL$ and using the Fubini-Tonelli theorem, we obtain

$$\begin{aligned} rn_\alpha(r) &= \int_{\mathbb{R}}\left(\int_{\mathbb{R}} \Gamma\big(\psi(r), r, w, L\big)\, g_\alpha^b(w)\left(1 + \mathbb{1}_{w^2 + \frac{L^2}{r_b^2} < 2\overline{\mathcal{U}_L}[\psi]}\right)\mathbb{1}_{r \geq r[\psi](L, w^2/2 + L^2/2r_b)}\, dw\right)\delta_{L=0}dL \\ &= \int_{\mathbb{R}} \Gamma\big(\psi(r), r, w, 0\big)\, g_\alpha^b(w)\left(1 + \mathbb{1}_{w^2 < 2\overline{\mathcal{U}_0}[\psi]}\right)\mathbb{1}_{r \geq r[\psi](0, w^2/2)}\, dw. \end{aligned}$$

Using now the fact that for $L = 0$

$$\forall r \in [1, r_b], \quad U_0[\psi](r) = \psi(r),$$

one obtains on the one hand $\overline{\mathcal{U}_0}[\psi] = \max\limits_{r \in [1, r_b]} \psi(r)$ and on the other hand using the definition (11) that $r[\psi]\,(0, w^2/2) = \widetilde{\rho}[\psi - w^2/2]$. For the ions one has $\psi = \phi$ and since $\phi$ is increasing on $[1, r_b]$ with $\phi(r_b) = 0$ it yields $\overline{\mathcal{U}_0}[\psi] = 0$. Thus, the first indicator function vanishes because the set $\big\{w \in \mathbb{R} \,:\, w^2 < \overline{\mathcal{U}_0}[\psi]\big\}$ is empty. For the second indicator function, one uses that the function $r \in [1, r_b] \longmapsto \phi(r) - w^2$ is increasing. Therefore we obtain on the one hand,

$$\mathbb{1}_{r \geq r[\psi](0, w^2/2)} \neq 0 \Longleftrightarrow r \geq \widetilde{\rho}[\phi - w^2/2] \Longleftrightarrow \phi(r) - \frac{w^2}{2} \leq 0 \Longleftrightarrow w^2 \geq 2\phi(r).$$

On the other hand, using the definition (19) we have

$$\Gamma\big(\psi(r), r, w, 0\big) \neq 0 \Longleftrightarrow w < 0 \text{ and } w^2 \geq 2\phi(r) \Longleftrightarrow w \geq 0.$$

Combining these two equivalences and the fact that $\phi(r) \leq 0$, we obtain exactly

$$\Gamma\big(\psi(r), r, w, 0\big)\,\mathbb{1}_{r \geq r[\psi](0, w^2/2)} \neq 0 \Longleftrightarrow w < 0.$$

This yields the formula (35). For the electrons, similar arguments and eventually using the change of variable $w = -\sqrt{v^2 - 2\phi(r)}$ yields the formula (36). For the current densities the proof is trivial. □

As explained at the beginning of this section, because of the formation of sheath the potential is expected to be increasing and such that locally near the probe ($r = 1$) the charge is positive. Owing to the corollary 4.2, we therefore see that the Poisson problem with radial incoming distributions (24) and with an increasing potential becomes a local semi-linear elliptic boundary value problem. Namely, we look for an increasing function $\phi : [1, r_b] \to \mathbb{R}$ solution to

$$-\lambda^2 \frac{d}{dr}\left(r\frac{d\phi}{dr}\right)(r) = q_i\big(\phi(r)\big) - q_e(\phi(r)), \quad r \in (1, r_b), \tag{40}$$

which satisfies the Dirichlet boundary conditions (8) and where the two functions $q_i : [\phi_p, 0] \to \mathbb{R}_+$ and $q_e : [\phi_p, 0] \to \mathbb{R}_+$ are defined for all $\nu \in [\phi_p, 0]$ by

$$q_i(\nu) = \int_{-\infty}^{0} \frac{|w|}{\sqrt{w^2 - 2\nu}} g_i^b(w)\, dw, \tag{41}$$

$$q_e(\nu) = \int_{-\infty}^{\sqrt{2(\nu-\phi_p)}} g_e^b\left(-\sqrt{v^2 - 2\nu}\right) dv. \tag{42}$$

For the sake of conciseness, we will restrict the analysis to the case $\phi_p < 0$ though the other case could be treated with similar ideas by simply changing the sign of the potential and switching the role of each species. Because of the sheath phenomena, the physical solution is expected to be such that $q_i(\phi(r)) > q_e(\phi(r))$ locally near the probe $r = 1$ while $q_i(\phi(r)) \approx q_e(\phi(r))$ in the core plasma at $r > r_b$. However this property cannot be true in general. We shall thus identify a class of incoming distribution functions for which $q_i - q_e$ is non negative everywhere in the interval $[\phi_p, 0]$. In this regard, we now assume that the boundary data $g_i^b$ and $g_e^b$ are such that the plasma core is locally neutral. We thus assume $n_i(r_b) = n_e(r_b)$ which is now equivalent to $q_i(0) = q_e(0)$. We are then led to the following first condition:

$$\int_{-\infty}^{0} g_i^b(w)dw = \int_{-\infty}^{0} g_e^b(w)dw + \int_{0}^{\sqrt{-2\phi_p}} g_e^b(-w)dw. \tag{43}$$

The rest of this section will be devoted to prove the following theorem.

**Theorem 4.3.** *Let $\phi_p < 0$ and $\lambda > 0$. Let $g_i^b : \mathbb{R}_-^* \longrightarrow \mathbb{R}^+$ and $g_e^b : \mathbb{R}_-^* \longrightarrow \mathbb{R}^+$ two incoming distribution functions having the integrability properties* (27)*. Additionally assume the following conditions.*

- *The plasma core is neutral: that is the incoming distribution functions $g_i^b$ and $g_e^b$ verify* (43)*.*
- *The incoming distribution function $g_e^b$ belongs to the Sobolev space $W^{2,1}(\mathbb{R}_-)$ and verifies for almost every $w < 0$, the two following differential inequalities:*

$$\frac{d}{dw}(g_e^b(w)e^{w^2}) \leq 0, \tag{44}$$

$$\frac{d}{dw}\left(\frac{1}{w}\frac{dg_e^b}{dw}(w)\right) + 2\frac{dg_e^b}{dw}(w) + wg_e^b(w) \geq 0. \tag{45}$$

- *The incoming distributions functions* $g_i^b$ *and* $g_e^b$ *verify the generalized Bohm condition:*

$$\int_{-\infty}^{0} \frac{g_i^b(w)}{w^2} dw < g_e^b\left(-\sqrt{-2\phi_p}\right)(-2\phi_p)^{-\frac{1}{2}} + \int_{-\infty}^{\sqrt{-2\phi_p}} \frac{dg_e^b}{dw}(-|v|)\frac{dv}{|v|}. \tag{46}$$

*Then, the Poisson equation* (40) *with the boundary conditions* (8) *admits a solution* $\phi_\lambda \in \mathcal{C}^2[1, r_b]$ *which is such that:*

- *It is increasing concave on* $[1, r_b]$.

- $\phi_\lambda$ *converges locally uniformly to zero on* $(1, r_b]$ *as* $\lambda \longrightarrow 0$. *Moreover, one has the estimate as* $\lambda \longrightarrow 0$*:*

$$\frac{\lambda^2}{2}\int_1^{r_b} r\left|\frac{d\phi_\lambda}{dr}(r)\right|^2 dr + \frac{\alpha}{2}\int_1^{r_b} |\phi_\lambda(r)|^2 dr \underset{\lambda\longrightarrow 0}{=} \mathcal{O}(\lambda), \tag{47}$$

  *where* $\alpha > 0$ *is constant independent of* $\lambda$. *Consequently, one has the quasi-neutral limit*

$$\|rn_i - rn_e\|_{L^1(1,r_b)} \underset{\lambda\longrightarrow 0}{\longrightarrow} 0\ . \tag{48}$$

- *There exists a constant* $C > 0$ *such that the following exponential decay estimate holds:*

$$\phi_p\, e^{-C\frac{r-1}{\lambda\sqrt{r_b}}} \ \leq\ \phi_\lambda(r)\ \leq\ 0.$$

- *The triplet of functions* $(\phi_\lambda, f_i, f_e)$ *with* $f_\alpha$ *defined by* (25) *and* (26) *is a measure valued solution of the stationary Radial 2-species Vlasov Poisson boundary value problem* (1)-(8).

Let us comment on this theorem. The inequalities (44) and (45) required for the incoming electrons distribution function $g_e^b$ are, up to our knowledge, new. They are in particular satisfied when $g_e^b$ is a semi-Maxwellian. These differential inequalities are used to prove the concavity of the function $\nu \in [\phi_p, 0] \mapsto e^{-\nu} q_e(\nu)$. The *generalized Bohm condition* (46) with the neutrality of the charge at $r = r_b$ (43) are sufficient conditions for the charge density $\nu \in [\phi_p, 0] \mapsto q_i(\nu) - q_e(\nu)$ to be non negative everywhere. They also imply an important coercivity estimate with respect to the $L^2$-norm of the non linear source term of the Poisson equation (40) which yields the quantitative boundary layer estimate (47). This estimate is a typical boundary layer estimate: it expresses the fact that the potential varies strongly over a spatial scale of the order of $\lambda$ with a gradient which scales as $\frac{1}{\lambda}$. Also remarks that provided the right hand-side in the *generalized Bohm condition* (46) is finite and positive, the inequality then implies that $\frac{g_i^b(w)}{w^2} \in L^1(\mathbb{R}^-)$. Therefore the function $g_i^b$ cannot charge too much the slow radial velocities.

When the *generalized Bohm condition* (46) is not verified, it is again possible to prove the existence of increasing solutions. It yields however another boundary layer estimate (47) where the zero-th order approximation of the solution $\phi_\lambda$ turns out to be an other value $\phi_0 \in [\phi_p, 0)$ such that $(q_i - q_e)(\phi_0) = 0$.

*4.2. Variational setting*

In this section, we recast the Poisson problem (40) as a minimization problem. So we firstly define the potential

$$\forall \nu \in [\phi_p, 0],\ \mathcal{Q}(\nu) = -\left( \int_0^{\nu} q_i(\nu') - q_e(\nu') d\nu' \right). \tag{49}$$

Using the Lebesgue dominated convergence theorem, it is not difficult to prove that if the incoming distributions $g_i^b$ and $g_e^b$ verify (27), the potential $\mathcal{Q}$ has the following properties:

$$\bullet\ \mathcal{Q} \in C^1[\phi_p, 0], \tag{50}$$

$$\bullet\ \forall \nu \in [\phi_p, 0], \quad \frac{d\mathcal{Q}}{d\nu}(\nu) = q_e(\nu) - q_i(\nu), \tag{51}$$

$$\bullet\ \frac{d\mathcal{Q}}{d\nu}(0) = 0. \tag{52}$$

We recall that the third property on the potential $\mathcal{Q}$ is equivalent to the neutrality in the plasma core (43). We now set the functional setting. We are going to work in the Sobolev space of $L^2$ functions on $[1, r_b]$ with $L^2$ derivatives, noted $V := H^1(1, r_b)$. In view of the radial Poisson problem (40), it is natural to equip this space with the weighted (quasi) scalar-product :

$$\langle \phi, \psi \rangle_V := \int_1^{r_b} \frac{d\phi}{dr}(r)\, \frac{d\psi}{dr}(r)\, r\, dr. \tag{53}$$

We also define the subspace:

$$V_0 = \{ v \in V,\ v(r_b) = 0 \}. \tag{54}$$

Remark now that for $\phi \in V_0$ one has,

$$\forall r \in [1, r_b], \quad \phi(r)^2 = -2 \int_r^{r_b} \frac{1}{\sqrt{r'}}\, \phi(r')\, \frac{d\phi}{dr}(r')\, \sqrt{r'}\, dr' \ \leq\ \frac{2}{\sqrt{r}} \int_r^{r_b} \left|\phi(r')\right| \left| \frac{d\phi}{dr}(r') \right| \sqrt{r'}\, dr'.$$

Using the Cauchy-Schwarz inequality yields the quantitative decay inequality

$$|\phi(r)|^2 \leq \frac{2}{\sqrt{r}} \left( \int_1^{r_b} |\phi(r')|^2 dr' \right)^{\frac{1}{2}} \left( \int_1^{r_b} r' \left| \frac{d\phi}{dr}(r') \right| dr' \right)^{\frac{1}{2}}. \tag{55}$$

Integrating on $[1, r_b]$ the inequality (55) gives the Poincaré inequality for $V_0$:

$$\left\| \phi \right\|_{L^2(1,r_b)} \leq 4(\sqrt{r_b} - 1) \left\| \sqrt{r}\, \frac{d\phi}{dr} \right\|_{L^2(1,r_b)} = 4(\sqrt{r_b} - 1)\, \left\| \phi \right\|_V. \tag{56}$$

This shows in particular that $V_0$ equipped with the scalar-product (53) is a Hilbert space. It is a consequence of a Sobolev embbeding that the convergence in $V_0$ implies the convergence in $\mathcal{C}^0$. We see that to evaluate the densities $q_i(\phi(r))$ and $q_e(\phi(r))$ for some $r \in (1, r_b)$, it is necessary that $\phi(r)$ belongs to the interval $[\phi_p, 0]$. So we restrict the set of admissible solutions to be

$$\mathcal{C} := \{ v \in V_0\ :\ v(1) = \phi_p < 0,\ \forall r \in [1, r_b], \phi_p \leq v(r) \leq 0\ \} \tag{57}$$

which is a closed convex subset of $V_0$. We eventually consider the minimization problem:

$$\text{Find} \quad \phi^* \in \mathcal{C} \quad \text{such that} \quad \mathcal{J}(\phi^*) = \inf_{\phi \in \mathcal{C}} \mathcal{J}(\phi), \tag{58}$$

where the functional $\mathcal{J}$ is defined by

$$\forall \phi \in \mathcal{C}, \quad \mathcal{J}(\phi) = \int_1^{r_b} \left( \frac{\lambda^2}{2} r |\phi'(r)|^2 + \mathcal{Q}(\phi(r)) \right) dr. \tag{59}$$

The functional $\mathcal{J}$ is a well-defined functional and of class $\mathcal{C}^1$ on $\mathcal{C}$. Its Fréchet differential is defined for any $\phi \in \mathcal{C}$ by

$$\begin{array}{rccc} d\mathcal{J}(\phi): & H_0^1[1, r_b] & \longrightarrow & \mathbb{R} \\ & h & \longmapsto & \displaystyle\int_1^{r_b} \lambda^2 r \frac{d\phi}{dr}(r) \frac{dh}{dr}(r) + \mathcal{Q}'(\phi(r)) h(r) dr. \end{array} \tag{60}$$

Critical points of $\mathcal{J}$ are functions $\phi \in \mathcal{C}$ such that $d\mathcal{J}(\phi)$ is identically zero. These are functions which are weak solutions to the Poisson equation (40).

We first prove the existence of minimizers.

**Proposition 4.4** (Existence of minimizers)**.** *Let $\mathcal{Q}$ given by* (49) *which satisfies* (50)-(52)*. Then, for any $\lambda > 0$ the functional $\mathcal{J}$ admits a minimizer on $\mathcal{C}$.*

*Proof.* Since $\mathcal{Q}$ is lower bounded, one has the following coercivity inequality:

$$\forall \phi \in \mathcal{C}, \quad \mathcal{J}(\phi) \geq \frac{\lambda^2}{2} \|\phi\|_V^2 + \inf_{\nu \in [\phi_p, 0]} \mathcal{Q}(\nu)(r_b - 1).$$

Let $(\phi_n)_{n \in \mathbb{N}} \subset \mathcal{C}$ be a minimizing sequence. As a consequence of this coercivity inequality, the sequence $(\phi_n)_{n \in \mathbb{N}}$ is bounded in $V_0$. Since $V_0$ is continuously embedded in $H^1(1, r_b)$, the sequence $(\phi_n)_{n \in \mathbb{N}}$ is also bounded in $H^1(1, r_b)$. Moreover because the embedding $H^1(1, r_b) \hookrightarrow \mathcal{C}^0[1, r_b]$ is compact, there exists $\phi^* \in V_0$ such that up to the extraction of a subsequence :

$$\phi_n \longrightarrow \phi^* \text{ weakly in } V_0, \qquad \phi_n \longrightarrow \phi^* \text{ in } \mathcal{C}^0[1, r_b], \qquad \text{as } n \to +\infty.$$

By convexity of the set $\mathcal{C}$, $\phi^* \in \mathcal{C}$. One has besides for all $n \in \mathbb{N}$, and $r \in [1, r_b]$:

$$|\mathcal{Q}(\phi_n(r)) - \mathcal{Q}(\phi^*(r))| = \left| \int_{\phi^*(r)}^{\phi_n(r)} q_e(\nu) - q_i(\nu) d\nu \right| \leq |\phi_n(r) - \phi^*(r)| \sup_{\nu \in [\phi_p, 0]} |q_e(\nu) - q_i(\nu)|. \tag{61}$$

This previous inequality yields the convergence $\displaystyle\int_1^{r_b} \mathcal{Q}(\phi_n(r)) dr \underset{n \to +\infty}{\longrightarrow} \int_1^{r_b} \mathcal{Q}(\phi^*(r)) dr$ because $(\phi_n)_{n \in \mathbb{N}}$ converges uniformly towards $\phi^*$. Using now the continuity and the convexity of the $H^1$-norm implies that it is lower semi-continuous with respect to the weak convergence. One concludes $\mathcal{J}(\phi^*) = \inf_{\phi \in \mathcal{C}} \mathcal{J}(\phi)$. □

We proved the existence of minimizers on the convex set $\mathcal{C}$. However, it is not granted that these minimizers are actually critical points of $\mathcal{J}$. It is because at the boundary of $\mathcal{C}$ the first order condition for a minimizer is in general a inequality (see [17] for the general theory).

*4.3. Concave increasing solutions*

In this section we give general sufficient conditions on $g_i^b$ and $g_e^b$ so that the minimizers of $\mathcal{J}$ on $\mathcal{C}$ are actually concave increasing solutions to (40). These conditions include in particular the so-called *generalized Bohm condition* of plasma physics [14].

*4.3.1. Study of the non linear term: a concavity property*

We begin first with the following lemma. Because we want our study to be generic, this lemma assumes technical differential inequalities on the electronic distribution function $g_e^b$. These differential inequalities are in particular satisfied when considering semi-Maxwellian distribution function for the electrons that is for $w < 0$, $g_e^b(w) = e^{-\frac{w^2}{2}}$.

**Lemma 4.5** (Concavity lemma)**.** *Let $g_e^b$ be a non negative function in the Sobolev space $W^{2,1}(\mathbb{R}_-)$. Assume it moreover satisfies for almost every $w < 0$ the two differential inequalities* (44) *and* (45)*. Define $q_e$ with* (42)*. Then the function $\mathcal{G}_e : \nu \mapsto e^{-\nu} q_e(\nu)$ belongs to $C^0[\phi_p, 0] \cap C^2(\phi_p, 0]$ and is concave.*

*Proof. Step 1: Regularity.* Concerning the continuity of $\mathcal{G}_e$ on $[\phi_p, 0]$, it is a direct consequence of the continuity of $g_e^b$ and of the definition of $q_e$ given at (42). We now prove that $\mathcal{G}_e$ has regularity $\mathcal{C}^2$ on $(\phi_p, 0]$. We recall that $g_e^b$ belongs to $W^{2,1}(\mathbb{R}_-) \subseteq \mathcal{C}^1(\mathbb{R}_-)$. Thus:

$$(\nu, v) \longmapsto g_e^b\Big( - \sqrt{v^2 - 2\nu}\Big) \in \ \mathcal{C}^1(D_1),$$

where $D_1 := \{(v, s) \in \mathbb{R}^2 : v^2 > 2\nu\}$. This implies, by integration,

$$(\nu, t) \longmapsto \int_{-\infty}^{\sqrt{2(t-\phi_p)}} g_e^b\left(-\sqrt{v^2 - 2\nu}\right) dv \quad \in \mathcal{C}^2(D_2),$$

where $D_2 := \{(\nu, t) \in \mathbb{R}^2 : t > \phi_p \text{ and } t > \phi_p + \nu\}$. This eventually gives the regularity of $q_e$ and hence of $\mathcal{G}_e$.

*Step 2: Concavity.* We establish its concavity by computing its second derivative. For all $\nu \in (\phi_p, 0]$ one has

$$\frac{d^2\mathcal{G}_e}{d\nu^2}(\nu) = e^{-\nu}\left(\frac{d^2 q_e}{d\nu^2}(\nu) - 2\frac{dq_e}{d\nu}(\nu) + q_e(\nu)\right).$$

We compute the derivative of $q_e$. Using the chain rule we obtain

$$\frac{dq_e}{d\nu}(\nu) = g_e^b\left(-\sqrt{-2\phi_p}\right)(2(\nu - \phi_p))^{-\frac{1}{2}} - \int_{-\infty}^{\sqrt{2(\nu-\phi_p)}} \frac{dg_e^b}{dw}\left(-\sqrt{v^2 - 2\nu}\right)\frac{dv}{-\sqrt{v^2 - 2\nu}},$$

$$\begin{aligned}\frac{d^2 q_e}{d\nu^2}(\nu) = &-g_e^b\left(-\sqrt{-2\phi_p}\right)(2(\nu - \phi_p))^{-\frac{3}{2}} - \frac{dg_e^b}{d\nu}(-\sqrt{-2\phi_p})\frac{(2(\nu - \phi_p))^{-\frac{1}{2}}}{-\sqrt{-2\phi_p}} \\ &+ \int_{-\infty}^{\sqrt{2(\nu-\phi_p)}} \frac{d}{dw}\left(\frac{1}{w}\frac{dg_e^b}{dw}\right)\left(-\sqrt{v^2 - 2\nu}\right)\frac{dv}{-\sqrt{v^2 - 2\nu}}.\end{aligned}$$

We then get

$$
\begin{aligned}
e^{\nu}\frac{d^2\mathcal{G}_e}{d\nu^2}(\nu) &= -g_e^b(-\sqrt{-2\phi_p})(2(\nu-\phi_p))^{-\frac{3}{2}} \\
&- (2(\nu-\phi_p))^{-\frac{1}{2}}\left(\frac{dg_e^b}{dw}(-\sqrt{-2\phi_p})\frac{1}{-\sqrt{-2\phi_p}} + 2g_e^b\left(-\sqrt{-2\phi_p}\right)\right) \\
&+ \int_{-\infty}^{\sqrt{2(\nu-\phi_p)}}\left\{\frac{d}{dw}\left(\frac{1}{w}\frac{dg_e^b}{dw}\right)\left(-\sqrt{v^2-2\nu}\right)\frac{1}{-\sqrt{v^2-2\nu}}\right. \\
&\left.+ \frac{dg_e^b}{dw}\left(-\sqrt{v^2-2\nu}\right)\frac{2}{-\sqrt{v^2-2\nu}} + g_e^b\left(-\sqrt{v^2-2\nu}\right)\right\}dv.
\end{aligned}
$$

The first term is non positive because the function $g_e^b$ is non negative. The two other terms are also non positive because $g_e^b$ verifies the two differential inequalities (44), (45). □

*4.3.2. Non-negativity of the macroscopic density : the generalized Bohm condition*

We have the following result.

**Proposition 4.6** (Non negativity of the macroscopic density)**.** *Let $g_e^b$ be a non negative function in the Sobolev space $W^{2,1}(\mathbb{R}_-)$ that satisfies for almost every $w<0$ the two differential inequalities* (44) *and* (45)*. Let $g_i^b$ a non negative function in $L^1(\mathbb{R}_-)$. Assume it satisfies the neutrality condition* (43) *and the following generalized Bohm inequality* (46)*. Then the function $\nu\in[\phi_p,0]\mapsto q_i(\nu)-q_e(\nu)$, defined by* (41) *and* (42)*, is positive on $[\phi_p,0)$ and vanishes at $\nu=0$.*

*Proof.* It is by assumption (43) that the function $q_i(\nu)-q_e(\nu)$ vanishes at $\nu=0$. Concerning the sign, one has for all $\nu\in[\phi_p,0]$

$$
q_i(\nu)-q_e(\nu) = e^{\nu}\left(\int_{-\infty}^{0}|w|g_i^b(w)\frac{e^{-\nu}}{\sqrt{w^2-2\nu}}dw - e^{-\nu}q_e(\nu)\right).
$$

Note that for $w<0$ the function $\nu\in[\phi_p,0]\mapsto\frac{e^{-\nu}}{\sqrt{w^2-2\nu}}$ is $C^1$ on $[\phi_p,0]$ and convex. The function $\nu\mapsto -e^{-\nu}q_e(\nu)$ is $\mathcal{C}^1$ on $(\phi_p,0]$ and also convex by virtue of the Lemma 4.5. Using the fact that a convex function always lays above its tangent lines, we obtain in the particular case of the tangent at the abscissa $\nu=0$,

$$
\begin{aligned}
q_i(\nu)-q_e(\nu) &\geq e^{\nu}\left(\int_{-\infty}^{0}g_i^b(w)dw - \left(\int_{-\infty}^{0}g_e^b(w)dw + \int_0^{\sqrt{-2\phi_p}}g_e^b(-w)dw\right)\right) \\
&+ e^{\nu}\nu\left(-\int_{-\infty}^{0}g_i^b(w)dw + \left(\int_{-\infty}^{0}g_e^b(w)dw + \int_0^{\sqrt{-2\phi_p}}g_e^b(-w)dw\right)\right) \\
&e^{\nu}\nu\left(\int_{-\infty}^{0}\frac{g_i^b(w)}{w^2}dw - g_e^b\left(-\sqrt{-2\phi_p}\right)(-2\phi_p)^{-\frac{1}{2}} - \int_{-\infty}^{\sqrt{-2\phi_p}}\frac{dg_e^b}{dw}(|v|)\frac{dv}{|v|}\right).
\end{aligned}
$$

Because of the equality (43) the first two terms of the right hand side of the above inequality vanishes so that it eventually remains

$$q_i(\nu) - q_e(\nu) \geq e^{\nu}\nu \left( \int_{-\infty}^{0} \frac{g_i^b(w)}{w^2} dw - g_e^b\left(-\sqrt{-2\phi_p}\right)(-2\phi_p)^{-\frac{1}{2}} - \int_{-\infty}^{\sqrt{-2\phi_p}} \frac{dg_e^b}{dw}(-|v|)\frac{dv}{|v|} \right).$$

Using now (46), we get that the term in parenthesis is negative. This concludes the proof of the positivity since $\nu \leq 0$. □

Several remarks are in order about this result.

- In the inequality (46) the right hand side is non negative if for instance $g_e^b$ is an increasing function on $\mathbb{R}_-$. This is verified in the classical case of the Maxwellian distribution $g_e^b(w) = e^{-\frac{w^2}{2}}$.
- Note that the Bohm inequality is equivalent to $\frac{d^2\mathcal{Q}}{ds^2}(0) > 0$.
- The reverse inequality $\frac{d^2\mathcal{Q}}{ds^2}(0) < 0$ yields by continuity, the negativity of the function $q_i - q_e$ locally near $\nu = 0$. The case of equality $\frac{d^2\mathcal{Q}}{ds^2}(0) = 0$ does not permit a priori to determine the sign of $q_i - q_e$. It requires the sign of higher order derivatives of $\mathcal{Q}$ at $\nu = 0$.

*4.3.3. Coercivity properties of the non-linear term*

In view of the previous sign study, we now consider distribution functions $g_i^b$ and $g_e^b$ to be such that (43), (44), (45) and (46) hold. The potential $\mathcal{Q}$ now verifies:

$$\bullet\ \mathcal{Q} \in C^1[\phi_p, 0] \cap C^2(\phi_p, 0], \tag{62}$$

$$\bullet\ \forall \nu \in [\phi_p, 0), \quad \frac{d\mathcal{Q}}{d\nu}(\nu) = q_e(\nu) - q_i(\nu) < 0, \tag{63}$$

$$\bullet\ \mathcal{Q}(0) = 0, \quad \frac{d\mathcal{Q}}{d\nu}(0) = 0, \quad \frac{d^2\mathcal{Q}}{d\nu^2}(0) > 0. \tag{64}$$

The potential $\mathcal{Q}$ is therefore non negative decreasing with a local convexity property at $\nu = 0$. We define:

$$\alpha := \inf_{\nu \in [\phi_p, 0]} \frac{1}{\nu}\frac{d\mathcal{Q}(\nu)}{d\nu}, \qquad \text{and} \qquad \beta := \sup_{\nu \in [\phi_p, 0]} \frac{1}{\nu}\frac{d\mathcal{Q}(\nu)}{d\nu}. \tag{65}$$

**Lemma 4.7.** *The numbers $\alpha$ and $\beta$ are positive and finite.*

*Proof.* Since $\mathcal{Q}$ is $C^1[\phi_p, 0] \cap C^2(\phi_p, 0]$ and $d\mathcal{Q}/d\nu(0) = 0$, the function $\nu \in [\phi_p, 0) \mapsto (1/\nu)d\mathcal{Q}/d\nu$ extends by continuity at $\nu = 0$ and its limit is $d^2\mathcal{Q}/d\nu^2(0)$ which is positive by hypothesis. Since $d\mathcal{Q}/d\nu$ is negative on $[\phi_p, 0)$, the function $\nu \in [\phi_p, 0] \mapsto (1/\nu)d\mathcal{Q}/d\nu$ is therefore positive and continuous on $[\phi_p, 0]$. Then it reaches respectively its maximum and its minimum inside the compact $[\phi_p, 0]$, which eventually gives respectively $\alpha$ and $\beta$. □

The previous lemma yields the two following inequalities:

$$\forall \nu \in [\phi_p, 0], \quad \beta\nu \leq \frac{d\mathcal{Q}(\nu)}{d\nu} \leq \alpha\nu, \tag{66}$$

$$\forall \nu \in [\phi_p, 0], \quad \beta\frac{\nu^2}{2} \geq \mathcal{Q}(\nu) \geq \alpha\frac{\nu^2}{2}. \tag{67}$$

These two inequalities are used to compare the minimizers of $\mathcal{J}$ with minimizers of quadratic minimization problems. They are used to describe the solution of the non-linear problem and obtain asymptotic estimates.

*4.3.4. Existence of concave increasing solutions*

We begin with the following lemma.

**Lemma 4.8** (Existence of non decreasing minimizers)**.** *Let $\mathcal{Q}$ that verifies* (62)*,* (63)*,* (64)*. Then the minimizers of $\mathcal{J}$ on $\mathcal{C}$ are non decreasing functions.*

*Proof.* We prove this fact by contraposition. Let $\phi \in \mathcal{C}$. We assume that $\phi$ is decreasing and we prove that it is not a minimizer. There exists $1 < x < y < r_b$ such that $\phi(x) > \phi(y)$. Consider the point $a = \sup\{a' \geq x \,:\, \forall r \in [x, a'],\, \phi(r) \leq \phi(x)\}$. By continuity of the function $\phi$, the point $a \in [x, r_b]$ exists and verifies both $\phi(a) = \phi(x)$ and $x \neq a$. Define:

$$\widetilde{\phi}(r) = \begin{cases} \phi(r) \text{ if } r \notin [x, a], \\ \phi(x) \text{ if } r \in [x, a]. \end{cases}$$

It is direct to check that $\widetilde{\phi} \in V_0$ and

$$\int_1^{r_b} \left|\frac{d\widetilde{\phi}}{dr}(r)\right|^2 r\, dr = \int_{[1,r_b]\setminus[x,a]} \left|\frac{d\widetilde{\phi}}{dr}(r)\right|^2 r\, dr = \int_{[1,r_b]\setminus[x,a]} \left|\frac{d\phi}{dr}(r)\right|^2 r\, dr < \int_1^{r_b} \left|\frac{d\phi}{dr}(r)\right|^2 r\, dr. \tag{68}$$

On the other hand, because the function $\mathcal{Q}$ is non increasing,

$$\forall r \in [1, r_b], \quad \mathcal{Q}(\tilde{\phi}(r)) \leq \mathcal{Q}(\phi(r)).$$

It thus yields $\mathcal{J}(\tilde{\phi}) < \mathcal{J}(\phi)$ and then $\phi$ is not a minimizer of $\mathcal{J}$. □

The main result of this section is the following.

**Proposition 4.9** (Existence of concave increasing solutions)**.** *Let $\mathcal{Q}$ that verifies* (62)*,*(63)*,* (64)*. For any $\lambda > 0$, the Poisson equation* (40) *with boundary condition* (8) *admits a classical solution $\phi \in \mathcal{C}^2[1, r_b]$ increasing and strictly concave.*

*Proof. Step 1: Decomposition of the interval* $(1, r_b)$*.* Let $\lambda > 0$ and denote $\phi \in \mathcal{C}$ a minimizer of $\mathcal{J}$. Since $\phi$ minimizes $\mathcal{J}$, one has for any test function $h \in H_0^1([1, r_b])$ such that $\phi + h \in \mathcal{C}$, $\mathcal{J}(\phi + h) - \mathcal{J}(\phi) \geq 0$. Since $\mathcal{J}$ is of class $\mathcal{C}^1$ on $\mathcal{C}$ the previous inequality implies that for all $h \in H_0^1$ such that $\phi + h \in \mathcal{C}$ one has

$$\mathrm{d}\mathcal{J}(\phi)(h) \geq 0, \tag{69}$$

where $\mathrm{d}\mathcal{J}(\phi)$ is the Fréchet derivative of $\mathcal{J}$ at $\phi$ given by (92). We are going to prove the case of equality holds in (69) for any test function in $\mathcal{C}^1_c((1,r_b))$. Consider the sets $\mathcal{O} := \{r \in (1,r_b) \,:\, \phi_p < \phi(r) < 0\}$, $\mathcal{F}_1 = \{r \in (1,r_b) \,:\, \phi(r) = \phi_p\}$ and $\mathcal{F}_2 = \{r \in (1,r_b) \,:\, \phi(r) = 0\}$. Since $\phi \in \mathcal{C}$, one has the decomposition

$$(1,r_b) = \mathcal{O} \cup \mathcal{F}_1 \cup \mathcal{F}_2.$$

Since $\phi$ is non decreasing by Lemma 4.8, there exists $1 \leq a < b \leq r_b$ such that

$$\mathcal{O} = (a,b), \quad \mathcal{F}_1 = (1,a], \quad \mathcal{F}_2 = [b,r_b).$$

*Step 2: $\mathcal{F}_1$ is empty.* Argue by contradiction and assume $\mathcal{F}_1$ is not empty, then $a > 1$. Let $h \in \mathcal{C}^1_c(1,a)$ non negative. By definition, there exists $\tau > 0$ small enough such that $\phi + \tau h \in \mathcal{C}$. Therefore since $h$ is compactly supported in $(1,a)$, the inequality (69) yields

$$\lambda^2 \int_1^a \frac{d\phi}{dr}(r)\,\frac{dh}{dr}(r)\,r\,dr + \int_1^a \frac{d\mathcal{Q}}{d\nu}\big(\phi(r)\big)\,h(r)\,dr \geq 0.$$

Note that in the interval $(1,a)$, $\phi$ is constant and equal to $\phi_p$ therefore the first integral term vanishes, and in virtue of the inequality (63), one has $\mathcal{Q}'(\phi_p) < 0$. Therefore the previous inequality re-writes

$$\mathcal{Q}'(\phi_p)\int_1^a h(r)dr \geq 0 \Longleftrightarrow \int_1^a h(r)dr \leq 0.$$

The last inequality yields the contradiction since $h$ is non negative and arbitrary.

*Step 3: Case of equality on $\mathcal{O} \cup \mathcal{F}_2 = (1,r_b)$.* For $h \in V_0$ with support in $\mathcal{O}$, there exists $\tau > 0$ small enough such that $\phi + \tau h \in \mathcal{C}$ and $\phi - \tau h \in \mathcal{C}$. Therefore, the inequality (69) implies:

$$\forall h \in \mathcal{C}^1_c(\mathcal{O}), \quad \int_1^{r_b} \lambda^2 r\,\frac{d\phi}{dr}(r)\,\frac{dh}{dr}(r) + \frac{d\mathcal{Q}}{d\nu}\big(\phi(r)\big)\,h(r)\,dr = 0. \tag{70}$$

Since the function $d\mathcal{Q}/d\nu$ is bounded, the equality (70) yields

$$\forall\, r \in \mathcal{O}, \qquad -\lambda^2 \frac{d}{dr}\left(r\frac{d\phi}{dr}(r)\right) = -\frac{d\mathcal{Q}}{d\nu}\big(\phi(r)\big). \tag{71}$$

Concerning the set $\mathcal{F}_2$, we have $d\phi/dr = 0$ and $d\mathcal{Q}/dw = 0$ so that (70) still holds for functions $h \in \mathcal{C}^1_c(\mathcal{F}_2)$. Thus

$$\forall\, r \in \mathcal{F}_2, \qquad -\lambda^2 \frac{d}{dr}\left(r\frac{d\phi}{dr}(r)\right) = -\frac{d\mathcal{Q}}{d\nu}\big(\phi(r)\big). \tag{72}$$

Invoking now the standard elliptic estimates and since $\mathcal{Q}$ is $\mathcal{C}^1[\phi_p,0]$, we conclude that the function $\phi$ is $\mathcal{C}^2$ on $[1,b]$ and on $[b,r_b]$. Since all the manipulated quantities are continuous, we infer that the Poisson equation holds on the full interval $[1,r_b]$:

$$\forall\, r \in [1,r_b], \qquad -\lambda^2 \frac{d}{dr}\left(r\frac{d\phi}{dr}(r)\right) = -\frac{d\mathcal{Q}}{d\nu}\big(\phi(r)\big). \tag{73}$$

The function $\phi$ is then $\mathcal{C}^2$ on the full interval $[1, r_b]$.

*Step 4: $\mathcal{F}_2$ is empty.* Let $\psi \in \mathcal{C}^2[1, r_b]$ the solution to the linear Poisson problem

$$\begin{cases} -\lambda^2 \dfrac{d}{dr}\left(r\dfrac{d\psi}{dr}\right) + \beta\psi = 0 \text{ in } (1, r_b) \\ \psi(1) = \phi_p, \quad \psi(r_b) = 0. \end{cases} \tag{74}$$

Consider now the difference $e = \phi - \psi$. One has $e(1) = e(r_b) = 0$ and

$$\forall r \in (1, r_b), \quad -\lambda^2 \frac{d}{dr}\left(r\frac{de}{dr}\right)(r) + \frac{d\mathcal{Q}}{d\nu}\big(\phi(r)\big) - \beta\psi(r) = 0. \tag{75}$$

Using the inequality (66), we obtain that $e$ verifies for all $r \in (1, r_b)$ :

$$-\lambda^2 \frac{d}{dr}\left(r\frac{de}{dr}\right)(r) + \beta e(r) \leq 0 \tag{76}$$

where $\beta > 0$. Invoking now a maximum principle one deduces that for all $r \in [1, r_b]$, $e(r) \leq 0$ which is equivalent to $\phi(r) \leq \psi(r)$. It is a standard result that the exact solution of the linear Poisson problem (74) verifies $\psi(r) < 0$ for all $r \in [1, r_b)$. It therefore implies that $\phi$ is negative on $[1, r_b)$ and thus $\mathcal{F}_2$ is empty.

*Step 5: Conclusion of the proof.* We proved that the solution $\phi$ to (73) exists and is $\mathcal{C}^2$, increasing and strictly concave on $\mathcal{O}$. We finally proved that $\mathcal{O} = (1, r_b)$, which gives the theorem. □

*4.3.5. Boundary layer estimates*

In this section, we establish asymptotic estimates as $\lambda \longrightarrow 0$ given by the Theorem 4.3 and that the solutions $\phi_\lambda$ converges locally uniformly on $(1, r_b]$ to zero. We begin with the following lemma.

**Lemma 4.10.** *Let $(\phi_n)_{n\in\mathbb{N}}$ a sequence of non-decreasing non-positive functions on $[1, r_b]$. Assume that*

$$\int_1^{r_b} |\phi_n(x)|^2 dx \longrightarrow 0 \quad \text{as } n \to +\infty.$$

*Then, the sequence $(\phi_n)_{n\in\mathbb{N}}$ converges locally uniformly to zero on the interval $(1, r_b]$.*

*Proof.* Since the functions $\phi_n$ are non-decreasing and non-positive, for all $a \in (1, r_b]$,

$$\sup_{r\in[a,r_b]} |\phi_n(r)| = |\phi_n(a)| = \sqrt{\frac{1}{a-1}\int_1^a |\phi_n(a)|^2\, dr} \leq \sqrt{\frac{1}{a-1}\int_1^a |\phi_n(r)|^2\, dr} \longrightarrow 0.$$

□

We have finally the next proposition.

**Proposition 4.11** (Boundary layer estimates)**.** *Let $(\phi_\lambda)_{\lambda>0}$ a family of non decreasing minimizers on $\mathcal{C}$ of $\mathcal{J}$ defined by* (59)*. Then one has the following estimates as $\lambda \to 0^+$ :*

$$\frac{\lambda^2}{2}\int_1^{r_b} r\left|\frac{d\phi}{dr}(r)\right|^2 dr + \frac{\alpha}{2}\int_1^{r_b} |\phi(r)|^2 dr \underset{\lambda\to 0}{=} \mathcal{O}(\lambda). \tag{77}$$

*Proof. Step 1: Bounds on the energy.* Since for any $\lambda > 0$, $\phi_\lambda \in \mathcal{C}$ minimizes the functional $\mathcal{J}_\lambda$. One has for any test function $\psi \in \mathcal{C}$, $\mathcal{J}(\phi_\lambda) \leq \mathcal{J}(\psi)$. So, consider $\psi \in V_0$ the solution of the linear Poisson problem

$$\begin{cases} -\lambda^2 \dfrac{d}{dr}\big(r\dfrac{d\psi}{dr}\big) + \alpha\psi = 0, \text{ in } (1, r_b) \\ \psi(1) = \phi_p, \quad \psi(r_b) = 0, \end{cases} \tag{78}$$

where we recall that $\phi_p < 0$ and $\alpha > 0$. Multiplying this equation by $\psi$ and integrating gives

$$\int_1^{r_b} \frac{\lambda^2}{2} r \left|\frac{d\psi}{dr}(r)\right|^2 dr = -\frac{\lambda^2}{2}\phi_p \frac{d\psi}{dr}(1) - \int_1^{r_b} \frac{\alpha}{2}|\psi(r)|^2 dr.$$

Owing to the weak maximum principle, one has for all $r \in [1, r_b]$, $\phi_p \leq \psi(r) \leq 0$ and therefore $\psi \in \mathcal{C}$. The energy of $\psi$ is given by

$$\mathcal{J}(\psi) = -\frac{\lambda^2}{2}\phi_p \frac{d\psi}{dr}(1) - \int_1^{r_b} \frac{\alpha}{2}|\psi(r)|^2 dr + \int_1^{r_b} \mathcal{Q}(\psi) dr \leq -\frac{\lambda^2}{2}\phi_p \psi'(1) + \frac{(\beta-\alpha)}{2}\int_1^{r_b} |\psi(r)|^2 dr,$$

where this last inequality is a consequence of (66). Combining this with (67) gives

$$\frac{\lambda^2}{2}\int_1^{r_b} r\left|\frac{d\phi}{dr}(r)\right|^2 dr + \frac{\alpha}{2}\int_1^{r_b} |\phi(r)|^2 dr \leq \mathcal{J}(\phi_\lambda) \leq \frac{\lambda^2}{2}\phi_p \frac{d\psi}{dr}(1) + \frac{(\beta-\alpha)}{2}\int_1^{r_b} |\psi(r)|^2 dr. \tag{79}$$

*Step 2: Asymptotic estimate for the solution of the linearized Poisson problem.* To obtain the asymptotic estimate (77), it is thus sufficient to estimate in the vicinity of $\lambda = 0$ the upper bound which is made of two terms. To do so, one uses the explicit solution of the linear Poisson problem (78) given by:

$$\forall r \in [1, r_b], \quad \psi(r) = \phi_p \left[ a(\lambda) I_0\left(\frac{2\sqrt{\alpha}}{\lambda}\sqrt{r}\right) + b(\lambda) K_0\left(\frac{2\sqrt{\alpha}}{\lambda}\sqrt{r}\right)\right], \tag{80}$$

where $I_0$ and $K_0$ are the first modified Bessel functions of the first and second kinds and the constants $a(\lambda)$ and $b(\lambda)$ are given by

$$a(\lambda) = \frac{-K_0\left(\frac{2\sqrt{\alpha}}{\lambda}\sqrt{r_b}\right)}{I_0\left(\frac{2\sqrt{\alpha}}{\lambda}\sqrt{r_b}\right) K_0\left(\frac{2\sqrt{\alpha}}{\lambda}\right) - K_0\left(\frac{2\sqrt{\alpha}}{\lambda}\sqrt{r_b}\right) I_0\left(\frac{2\sqrt{\alpha}}{\lambda}\right)},$$

$$b(\lambda) = \frac{I_0\left(\frac{2\sqrt{\alpha}}{\lambda}\sqrt{r_b}\right)}{I_0\left(\frac{2\sqrt{\alpha}}{\lambda}\sqrt{r_b}\right) K_0\left(\frac{2\sqrt{\alpha}}{\lambda}\right) - K_0\left(\frac{2\sqrt{\alpha}}{\lambda}\sqrt{r_b}\right) I_0\left(\frac{2\sqrt{\alpha}}{\lambda}\right)},$$

where the denominator is positive because the function $I_0$ is positive increasing and the function $K_0$ is positive decreasing. We now use classical asymptotic estimates (see [12]) for the modified Bessel functions as $z \to +\infty$ [12] :

$$I_0(z) \simeq \frac{e^z}{\sqrt{2\pi z}} \sum_{k=0}^{+\infty} \frac{a_k}{z^k}, \qquad K_0(z) \simeq \sqrt{\frac{\pi}{2z}}\, e^{-z} \sum_{k=0}^{+\infty} (-1)^k \frac{a_k}{z^k}, \qquad a_k := \frac{1}{k!\, 8^k} \prod_{j=0}^{k} (2j-1)^2.$$

Plugging these estimates in (80) gives the announced asymptotic expansion as $\lambda \to 0$. □

We finally prove the exponential decay estimate:

**Lemma 4.12** (Exponential decay)**.** *Let $\lambda > 0$ and let $\phi_\lambda$ be a non-decreasing concave minimizer on $\mathcal{C}$ of $\mathcal{J}$ defined by* (59)*. Then there exists $C > 0$ tel que*

$$\phi_p \exp\Big( - C\frac{r-1}{\lambda\sqrt{r_b}}\Big) \ \leq \ \phi_\lambda(r) \ \leq \ 0.$$

*Proof.* Using Estimate (66), we write from (40)

$$\begin{aligned} 0 &= -\frac{d^2\phi_\lambda}{dr^2} - \frac{1}{r}\frac{d\phi_\lambda}{dr} + \frac{1}{\lambda^2 r}\mathcal{Q}\big(\phi_\lambda(r)\big) \\ &\leq -\frac{d^2\phi_\lambda}{dr^2} - \frac{1}{r}\frac{d\phi_\lambda}{dr} + \frac{\alpha}{\lambda^2 r}\phi_\lambda(r) \\ &\leq -\frac{d^2\phi_\lambda}{dr^2} + \frac{\alpha}{\lambda^2 r_b}\phi_\lambda(r), \end{aligned} \tag{81}$$

where for the last inequality we used $\phi_\lambda$ negative increasing and $r \leq r_b$. We now remark that, when $A \geq 0$, the equation $d^2\phi/dr^2 = A\phi$ admits as solution the functions $r \mapsto B\, exp(-\sqrt{A}(r-1))$ as increasing solutions, where $B \leq 0$. We then deduce the announced estimate from the inequality above by invoking the maximum principle to compare the solutions of elliptic equations. □

The proof of Theorem 4.3 is then a straightforward consequence of Propositions 4.9 and 4.11 and of Lemmas 4.10 and 4.12.

## 5. The numerical method

We describe hereafter the numerical method that we use to solve the non linear and non local Poisson problem (3). From a numerical perspective, it is convenient to introduce the harmonic lifting of the boundary conditions. Namely, we consider $\widetilde{\phi} : [1, r_b] \to \mathbb{R}$ that verifies

$$-\lambda^2 \frac{d}{dr}\left( r\frac{d\widetilde{\phi}}{dr}\right)(r) = 0, \quad r \in (1, r_b) \tag{82}$$

with the Dirichlet boundary conditions

$$\widetilde{\phi}(1) = \phi_p, \quad \widetilde{\phi}(r_b) = 0. \tag{83}$$

It has the explicit formula given for all $r \in [1, r_b]$ by $\widetilde{\phi}(r) = \phi_p\left(1 - \frac{\ln(r)}{\ln(r_b)}\right)$. We finally consider the change of unknown $\psi = \phi - \tilde{\phi}$. Therefore the Poisson equation (23) of unknown $\phi$ is equivalent to the Poisson equation of unknown $\psi : [1, r_b] \to \mathbb{R}$,

$$-\lambda^2 \frac{d}{dr}\left( r\frac{d\psi}{dr}\right)(r) = \widetilde{n}[\psi](\psi(r), r), \quad r \in (1, r_b), \tag{84}$$

where $\widetilde{n}[\psi](\psi(r), r) = n\left[\psi + \tilde{\phi}\right]\left(\psi(r) + \tilde{\phi}(r), r\right)$ with the homogeneous Dirichlet boundary conditions

$$\psi(1) = 0, \quad \psi(r_b) = 0. \tag{85}$$

We describe hereafter how we solve (84) with a fixed-point approach based on a gradient descent method. Then we explain the finite element framework that is used to approximate the solutions and then explain how non local parameters are computed. Eventually, we briefly explain how integrals are numerically treated.

*5.1. A fixed point method based on the gradient descent method*

To solve the Poisson problem (84)-(85) we are going to use a gradient descent method. The first observation is that strong solutions $\psi$ to (84)-(85) are also weak solutions in the sense:

$$\forall h \in H_0^1[1, r_b], \quad \int_1^{r_b} \lambda^2 \frac{d\psi}{dr}(r)\frac{dh}{dr}(r)r - \widetilde{n}[\psi](\psi(r), r)h(r)dr = 0. \tag{86}$$

Note that because of the non-local terms, this variational formulation does not stem directly from the Euler-Lagrange equation of a functional. It is nevertheless the case if the non-local contribution $[\psi]$ is replaced by the contribution of a fixed function that one can see as a parameter. Indeed, let $u \in H_0^1[1, r_b]$ a given function and consider the auxiliary problem which consists in finding $\psi[u] \in H_0^1[1, r_b]$ such that

$$\forall h \in H_0^1[1, r_b], \quad \int_1^{r_b} \lambda^2 \frac{d\psi}{dr}(r)\frac{dh}{dr}(r)r - \widetilde{n}[u](\psi(r), r)h(r)dr = 0. \tag{87}$$

This non linear variational problem corresponds to the Euler-Lagrange equation of the functional $\mathcal{E}[u] : H_0^1[1, r_b] \to \mathbb{R}$ given by

$$\forall \psi \in H_0^1[1, r_b], \quad \mathcal{E}[u](\psi) = \int_1^{r_b} \frac{\lambda^2}{2}\left|\frac{d\psi}{dr}(r)\right|^2 r - \widetilde{N}[u](\psi(r), r)dr \tag{88}$$

where the non linear (and now local) term is given by

$$\widetilde{N}[u](\nu, r) = \int_0^{\nu} n[u](\nu', r)d\nu'. \tag{89}$$

With appropriate integrability assumption on the incoming data $f_i^b$ and $f_e^b$ (see Lemma 5.4 in [2]) there exists $\psi[u] \in H_0^1[1, r_b]$ which minimizes $\mathcal{E}[u]$ on $H_0^1[1, r_b]$. It is in particular a solution to the auxiliary problem (87). To solve the non local problem (86), we eventually consider the sequence $(\psi^n)_{n\in\mathbb{N}} \subset H_0^1[1, r_b]$ defined by induction as follows

$$\begin{cases} \psi^0 \in H_0^1[1, r_b], \\ \forall n \in \mathbb{N}, \quad \psi^{n+1} = \psi^n - \rho\nabla\mathcal{E}[\psi^n](\psi^n), \end{cases} \tag{90}$$

where the initial term of the sequence $\psi^0 \in H_0^1[1, r_b]$ is chosen freely, $\rho > 0$ is a fixed numerical parameter and the gradient $w[\psi^n] := \nabla\mathcal{E}[\psi^n](\psi^n) \in H_0^1[1, r_b]$ is the unique solution to the variational problem

$$\forall h \in H_0^1[1, r_b], \quad \langle w[\psi^n], h\rangle_V = d\mathcal{E}[\psi^n](\psi^n)(h) \tag{91}$$

where $\langle\cdot,\cdot\rangle_V$ is the scalar product defined in (53) and

$$\begin{array}{rccc} d\mathcal{E}[\psi^n](\psi^n) : & H_0^1 & \longrightarrow & \mathbb{R} \\ & h & \longmapsto & \displaystyle\int_1^{r_b} \lambda^2 \frac{d\psi^n}{dr}(r)\frac{dh}{dr}(r)r - \widetilde{n}[\psi^n](\psi^n(r), r)h(r)dr, \end{array} \tag{92}$$

is the Fréchet differential of $\mathcal{E}[\psi^n]$.

Using a uniform bound on the macroscopic densities $n_i$ and $n_e$, a Sobolev compact embedding, the Arzelà-Ascoli theorem and the Lebesgue dominated convergence theorem, we managed to prove [2], the existence of a subsequence that converges toward a solution of the stationary radial 2-species Vlasov-Poisson equation. Note however, that the convergence of the whole sequence is not guaranteed in general because the convexity properties of the functional $\mathcal{E}[u]$ are not known. Relying on the convergence study of the non local terms in [2], we nevertheless see that if the sequence $(\psi^n)_{n\in\mathbb{N}}$ converges towards some $\psi$ then $\nabla\mathcal{E}[\psi](\psi) = 0$. It means exactly that $\psi$ solves (86).

*5.2. Finite element approximation*

To approximate the solutions to (86), we use an affine finite element approximation. Let $N_{dof} \in \mathbb{N}$ and consider a uniform mesh of the interval $[1, r_b]$ made of interval of size $h = \frac{(r_b-1)}{N_{dof}+1}$. Namely, we subdivide the interval $[1, r_b]$ into $N_{dof} + 1$ intervals $[r_k, r_{k+1}]$ where the nodes are given for all integer $k = 0, ..., N_{dof} + 1$, by $r_k = 1 + kh$. We consider the affine finite element subspace of $H^1_0[1, r_b]$

$$V_{0,h} := \{\psi_h \in \mathcal{C}^0[1, r_b] \ : \ \psi(1) = 0, \ \psi(r_b) = 0 \ : \ \forall k \in \{0, ..., N_{dof}\} \ \psi_{h|[r_k,r_{k+1}]} \text{ is affine } \}. \quad (93)$$

It is a finite dimensional space of dimension $N_{dof}$. To approximate the solutions to (86) we then use the approximate gradient descent method which consists in considering the sequence of approximate solutions $(\psi^n_h)_{n\in\mathbb{N}} \subset V_{0,h}$ defined by induction as follows

$$\begin{cases} \psi^0 \in V_{0,h}, \\ \forall n \in \mathbb{N}, \quad \psi^{n+1}_h = \psi^n_h - \rho\nabla\mathcal{E}[\psi^n_h](\psi^n_h), \end{cases} \quad (94)$$

where the initial term of the sequence $\psi^0_h \in V_{0,h}$ is chosen freely, $\rho > 0$ is a fixed numerical parameter and the gradient $w[\psi^n_h] := \nabla\mathcal{E}[\psi^n_h](\psi^n_h) \in V_{0,h}$ solves the variational problem (91) where the space $H^1_0[1, r_b]$ is replaced by the subspace $V_{0,h}$. A standard basis of the space $V_{0,h}$ is the family of the so called *hat functions* given for all integer $k = 1, .., N_{dof}$ by

$$\hat{\psi}_k(r) = \mathbb{1}_{[r_{k-1},r_k]}(r)\frac{(r - r_k)}{h} + \mathbb{1}_{[r_k,r_{k+1}]}(r)\frac{(r_{k+1} - r)}{h}. \quad (95)$$

Using this basis, solving (91) in $V_{0,h}$ reduces to solve a linear invertible system of $N_{dof}$ equations. The stiffness matrix associated with the scalar product (53) is of size $N_{dof} \times N_{dof}$ and is given for $(k, l) \in \{1, ..., N_{dof}\}^2$ by $A_{kl} = \langle\hat{\psi}_l, \hat{\psi}_k\rangle_V$. It has an explicit expression and it is a symmetric positive definite matrix. It can be computed and inverted only once so that the cost of computing the gradient at each iterate in the approximate gradient descent method (94) is the cost of inverting the matrix once and computing a matrix-vector product at each iterate. Standard results concerning the convergence of the sequence of approximate solutions (both as $h \to 0$ and $n \to +\infty$) in the simplified case where $\mathcal{E}[\psi]$ is a uniformly convex functional can be found in [9].

*5.3. Computing the gradient*

To compute the gradient $\nabla\mathcal{E}[\psi_h^n](\psi_h^n)$ at each iterate $n \in \mathbb{N}$ of the sequence (94), one needs to compute the right hand side which is a vector of $\mathbb{R}^{N_{dof}}$ whose components in the basis $\{\hat{\psi}_k\}_{k=1,...,N_{dof}}$ are given for all integer $k = 1, .., N_{dof}$ by

$$g_k = d\mathcal{E}[\psi_h^n](\hat{\psi}_k), \tag{96}$$

where $d\mathcal{E}[\psi_h^n](\hat{\psi}_k)$ is given by the formula (92). This formula is made of two terms: the first term $\displaystyle\int_1^{r_b} \lambda^2 \frac{d\psi_h^n}{dr}(r)\frac{d\hat{\psi}_k}{dr}(r)rdr$ can be computed explicitly because $\psi_h^n$ is piecewise affine. The second term $\displaystyle\int_1^{r_b} \widetilde{n}[\psi_h^n](\psi_h^n(r), r)\hat{\psi}_k(r)dr$ cannot a priori be computed explicitly. It requires a numerical integration in the space variable $r$ and also in the velocity space $(v_r, v_\theta)$. It also needs the numerical computation of the non local terms $\overline{\mathcal{U}_L}[\psi_h^n]$, $\widetilde{\rho}\Big[\psi_h^n + \frac{L^2}{2}\Big(\frac{1}{\bullet^2} - \frac{1}{r_b^2}\Big) - w^2\Big]$. So we shall describe here after the numerical procedure to compute this second term.

*5.3.1. Approximate max-parameter*

Assume the $n$-th term of the sequence $\psi_h^n \in V_{0,h}$ to be known. To approximate the *max parameter* $\overline{\mathcal{U}_L}[\psi_h^n]$ for each $L \in \mathbb{R}$, we use the standard projection operator

$$\begin{array}{rccc} \pi_h : & \mathcal{C}^0[1, r_b] & \longrightarrow & V_h \\ & \psi & \mapsto & \pi\psi \end{array} \tag{97}$$

where $V_h$ is the $N_{dof} + 2$ dimensional subspace of $H^1[1, r_b]$ given by

$$V_h := \{\psi \in \mathcal{C}^0[1, r_b] \ : \forall k \in \{0, ..., N_{dof}\}\ \psi_{h|[r_k, r_{k+1}]} \text{ is affine}\}. \tag{98}$$

Then for each $L \in \mathbb{R}$, the function $\mathcal{U}_L[\psi_h^n]$ given by (9) is projected onto $V_h$ and we approximate $\overline{\mathcal{U}_L}[\psi_h^n]$ by $\overline{\pi_h\left(\mathcal{U}_L[\psi_h^n]\right)}$. Since $\pi_h\left(\mathcal{U}_L[\psi_h^n]\right)$ is a continuous and piecewise affine interpolation of $\mathcal{U}_L[\psi_h^n]$ , one has

$$\overline{\pi_h\left(\mathcal{U}_L[\psi_h^n]\right)} = \max\left\{\mathcal{U}_L[\psi_h^n](r_k) \ : \ k = 0, .., N_{dof} + 1\right\}. \tag{99}$$

Eventually, one remarks that if $\psi_h^n$ converges uniformly towards some function $\psi^n$ as $h \longrightarrow 0$, then $\pi_h\left(\mathcal{U}_L[\psi_h^n]\right) \longrightarrow \mathcal{U}_L[\psi^n]$ uniformly and by continuity of the *max-parameter* we also have $\overline{\pi_h\left(\mathcal{U}_L[\psi_h^n]\right)} \longrightarrow \overline{\mathcal{U}_L}[\psi^n]$.

*5.3.2. Approximate barrier-parameter*

For each $(w, L) \in \mathbb{R}^2$ we approximate $\widetilde{\rho}\big[\psi_h^n + \frac{L^2}{2}\big(\frac{1}{\bullet^2} - \frac{1}{r_b^2}\big) - w^2\big]$ by $\widetilde{\rho}\big[\pi_h\big(\psi_h^n + \frac{L^2}{2}\big(\frac{1}{\bullet^2} - \frac{1}{r_b^2}\big) - w^2\big)\big]$. In this approximation, the argument of $\widetilde{\rho}$ has been replaced by a continuous and piecewise affine function on $[1, r_b]$. Several strategies exist to compute $\widetilde{\rho}[\psi]$ for a fixed function $\psi \in V_h$. We propose the following simple one which consists in computing firstly

$$\tilde{k} = \tilde{k}[\psi] := \min\left\{k \in [\![0, N_{dof} + 1]\!] \ : \ \psi(r_{k'}) \leq 0 \quad \forall k' \in [\![k, N_{dof} + 1]\!]\right\}. \tag{100}$$

By definition, one has $\psi(r_{\tilde{k}-1}) > 0$ and $\psi(r_{\tilde{k}}) \leq 0$. Since the function $\psi$ is affine in the interval $[r_{\tilde{k}-1}, r_{\tilde{k}}]$ there is a unique $a \in [r_{\tilde{k}-1}, r_{\tilde{k}}]$ such that $\psi(a) = 0$ which can be explicitly

computed. So we set $\widetilde{\rho}(\psi) = a$. From the algorithmic point of view, it is worth noticing that $\widetilde{\rho}\big[\pi_h\big(\psi_h^n + \frac{L^2}{2}\big(\frac{1}{\bullet^2} - \frac{1}{r_b^2}\big) - w^2\big)\big]$ will be needed for several values of $(w, L) \in \mathbb{R}^2$ because of the integration in the velocity space. One can therefore use in addition the following monotony property:

$$\forall\, (\psi_1, \psi_2) \in V_h^2, \quad \psi_1 \leq \psi_2 \quad \Longrightarrow \quad \widetilde{\rho}[\psi_1] \leq \widetilde{\rho}[\psi_2]. \tag{101}$$

It yields that the associated integers to $\psi_1$ and $\psi_2$ verify $\tilde{k}[\psi_1] \leq \tilde{k}[\psi_2]$ and thus,

$$\tilde{k}[\psi_1] = \min\Big\{k \in [\![0, \tilde{k}[\psi_2]]\!] \,:\, \psi_1(r_{k'}) \leq 0 \quad \forall k' \in [\![k, \tilde{k}[\psi_2]]\!]\Big\}\,.$$

Thus, if for each $L \in \mathbb{R}$ the values of $w$ are ordered monotoneously, one can use the previous formula to avoid the redundancy of useless values.

*5.3.3. Numerical quadratures*

Let $\psi_h \in V_{0,h}$. We describe here briefly how we approximate the quantity $g_\alpha[\psi_h](\psi_h(r), r)$ for a given $r \in [1, r_b]$. The first step consists in localising the essential support of the incoming boundary data $f_\alpha^b$. More precisely, we consider $\varepsilon_m > 0$ and $(\bar{w}, \bar{L}) \in \mathbb{R}_- \times \mathbb{R}_+$ such that

$$(L, w) \notin [-\bar{L}, \bar{L}] \times [\bar{w}, 0] \Longrightarrow |f_\alpha^b(w, L/r_b)| < \varepsilon_m. \tag{102}$$

In practice, we take $\varepsilon_m$ being the machine relative zero. Then we approximate $g_\alpha[\psi_h](\psi_h(r), r)$ using the equivalent formulas (17) using a numerical integration on the rectangle $\mathcal{Q} := [0, \bar{L}] \times [\bar{w}, 0]$ where the *max-parameter* and the *barrier-parameter* are replaced by their approximation. One interest of the formula (17) is that it splits the integral (22) into two integrals where each integral has a clear physical meaning. Then the numerical integration in velocity uses high order Gauss-Lobatto quadratures.

Eventually for the computation of the gradient with the finite element approximation, the integrals in space are also treated with high order Gauss-Lobatto quadratures.

## 6. Numerical results

In the following numerical experiment, the incoming distributions data are chosen for $\alpha = i, e$ of the form

$$\forall (v_r, v_\theta) \in \mathbb{R}_-^* \times \mathbb{R}, \quad f_\alpha^b(v_r, v_\theta) = g_\alpha^b(v_r) \otimes \mathcal{M}_T(v_\theta) \tag{103}$$

where

$$\mathcal{M}_T(v_\theta) = \frac{1}{\sqrt{2\pi T}} e^{-\frac{v_\theta^2}{2T}} \tag{104}$$

is a *Maxwellian* distribution in the angular velocity variable with a temperature $T > 0$. For the computation of the electronic current density, the mass ratio is taken equal to $\mu = 1/3600$ which corresponds to the mass ratio of a Deuterium plasma. The normalized Debye length is taken equal to $\lambda = 0.1$. The exterior boundary radius is fixed to $r_b = 3$. For the finite element approximation the mesh size is taken equal to $h = 2/500$. For the computation of velocity and space integrals, we use a fifth order Gauss-Lobatto quadrature. Then for the gradient method (94),we proceed in two steps.

*First step :* We first solve the *radial* Poisson problem (40) by minimization of the functional $\mathcal{J}$. We take as initial guess $\psi_h^0$ being the null function. Then we stop the algorithm when there exists $n_0 \in \mathbb{N}$ such that $\|\nabla\mathcal{J}(\psi_h^{n_0})\|_{L^\infty} < 10^{-8}$.

*Second step :* If $T \neq 0$, we solve the non linear non local Poisson problem (84) by restarting the gradient method (94) with the initial guess $\psi_h^0 = \psi_h^{n_0}$ which corresponds to an approximate radial solution. We stop the algorithm at the first iterate such that $\|\nabla\mathcal{E}[\psi_h^n](\psi_h^n)\|_{L^\infty} < 10^{-4}$.

When $T \longrightarrow 0$, it is easy to prove that $\mathcal{M}_T \longrightarrow \delta_{v_\theta=0}$ in the sense of distribution. By virtue of the continuity properties (4.1) of the non linear source term, it is expected that the *radial solutions* are close to the *non radial solutions* when $T$ is close to zero. We propose two test cases. The first one concerns the computation of *radial solutions* which corresponds to the limit $T = 0$. According to the Theorem 4.3, we must observe when the *generalized Bohm condition* is verified that the computed electrostatic potential is concave increasing. The limit case $T = 0$ is therefore a benchmark to validate the numerical method. The second one is the computation of *non radial solutions* which correspond to small positive values of $T \neq 0$. This test case is prospective and we are mainly interested in the existence of effective potential barriers and on the description of the probe characteristic.

### *6.1. Radial solutions*

We consider the limit case $T = 0$. In the two following test cases the incoming distribution function for the electrons is a *Maxwellian* given by

$$\forall v_r < 0, \quad g_e^b(v_r) = \frac{n^b}{\sqrt{2\pi}} e^{-\frac{v_r^2}{2}}, \tag{105}$$

where $n^b > 0$ is a positive constant that is determined according the choice of the incoming distribution function $g_i^b$ such that the neutrality in the core plasma (43) is ensured.

#### *6.1.1. Case 1: satisfied Bohm condition*

For this test case the incoming distribution for the ions is given by

$$\forall v_r < 0, \quad g_i^b(v_r) = \frac{v_r^2}{\sqrt{2\pi}} e^{-\frac{(v_r-u_i)^2}{2}}, \tag{106}$$

where the value of $u_i < 0$ is chosen so that the *generalized Bohm condition* (46) is satisfied. We take here $u_i = -2.0$. In Figure 3 (left), we represent the potential $\phi(r)$, $r \in [1, r_b = 3]$, obtained for different values of the probe potential $\phi_p$. From Proposition 2.2 and quadrature formulas, we reconstruct the macroscopic ionic and electronic densities and represent in Figure 3 (right) the difference $rn_i(r) - rn_e(r)$. Same quantities are plotted in y-log scale in Figure 4. In Figure 5, we plot the macroscopic densities separately: $rn_i(r)$ on the left and $rn_e(r)$ on the right. We obtain the expected behavior of Theorem (4.3). We see that the potential is increasing concave and tends exponentially fast to *zero* away from the boundary $r = 1$ while a boundary layer of the order of the Debye length in size is observed near $r = 1$. Accordingly the sign of the charge density is everywhere non negative. There also seems to be some monotony with respect to the probe potential value $\phi_p$.

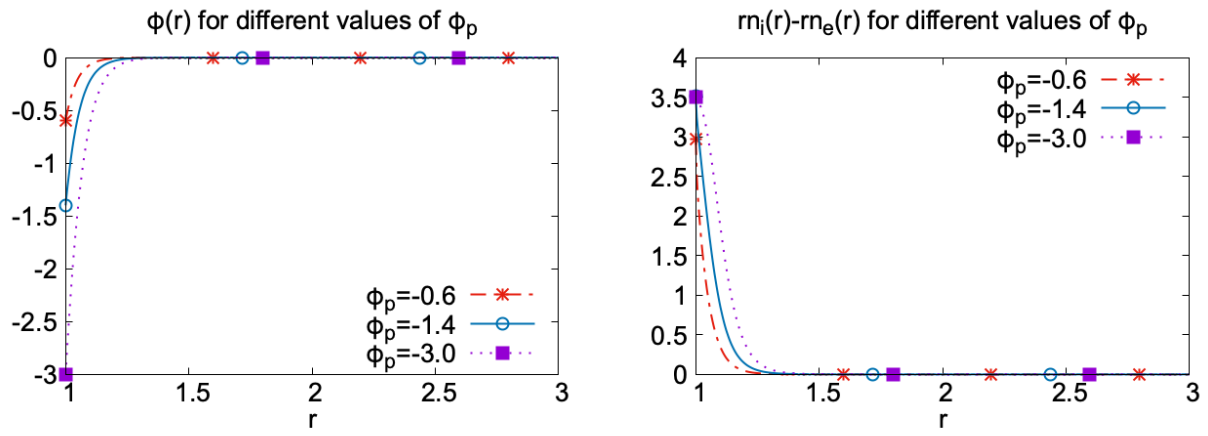


Figure 3: Radial case with satisfied Bohm condition: potential $\phi(r)$ (left) and density difference $rn_i(r) - rn_e(r)$ (right) for $\phi_p$ varying from $-0.6$ to $-3$.

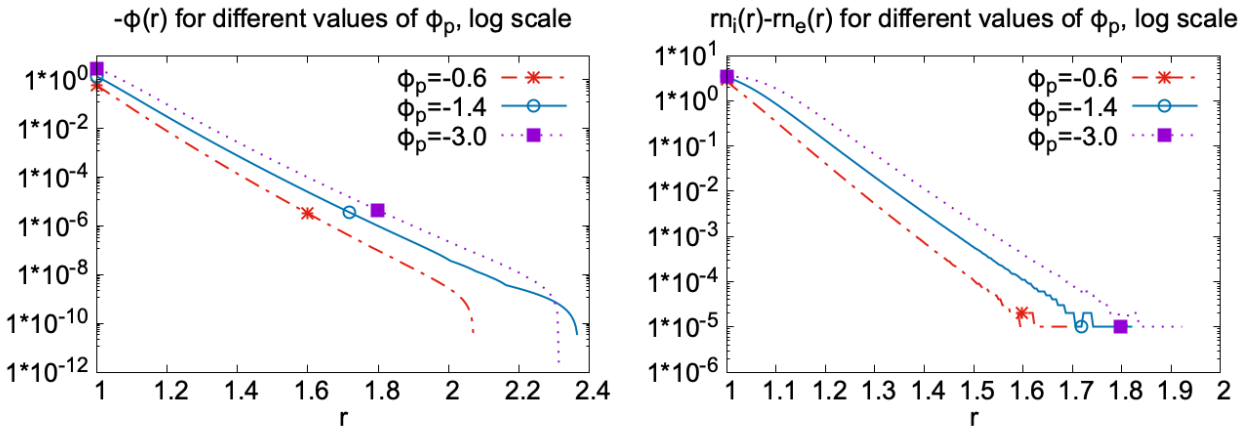


Figure 4: Radial case with satisfied Bohm condition: potential $\phi(r)$ (left) and density difference $rn_i(r) - rn_e(r)$ (right) for $\phi_p$ varying from $-0.6$ to $-3$. y-log scale.

### *6.1.2. Case 2: unsatisfied Bohm condition*

For this test case the incoming distribution for the ions is half a *Maxwellian*:

$$\forall v_r < 0, \quad g_i^b(v_r) = \frac{1}{\sqrt{2\pi}} e^{-\frac{v_r^2}{2}}. \tag{107}$$

It does not verify the *generalized Bohm condition* (46) because it does not vanish locally near $v_r = 0$. The potential and densities plots are strongly different from the previous case. We represent $\phi(r)$ (resp. $rn_i(r) - rn_e(r)$) on the left (resp. right) of Figure 6 and $rn_i(r)$ (resp. $rn_e(r)$) on the left (resp. right) of Figure 7. Again we see that the electrostatic potential is increasing but it has this time two boundary layers. We believe that the boundary layer at $r = r_b$ is unphysical. At least, there seems to be an incompatibility in this case with the neutrality condition $n_i(r_b) = n_e(r_b)$.

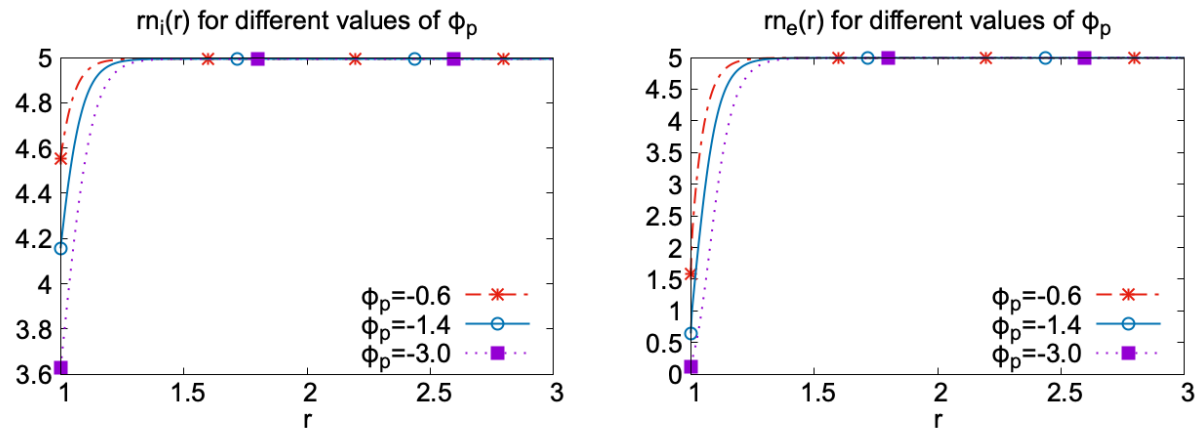


Figure 5: Radial case with satisfied Bohm condition: ionic density $rn_i(r)$ (left) and electronic density $rn_e(r)$ (right) for $\phi_p$ varying from $-0.6$ to $-3$.

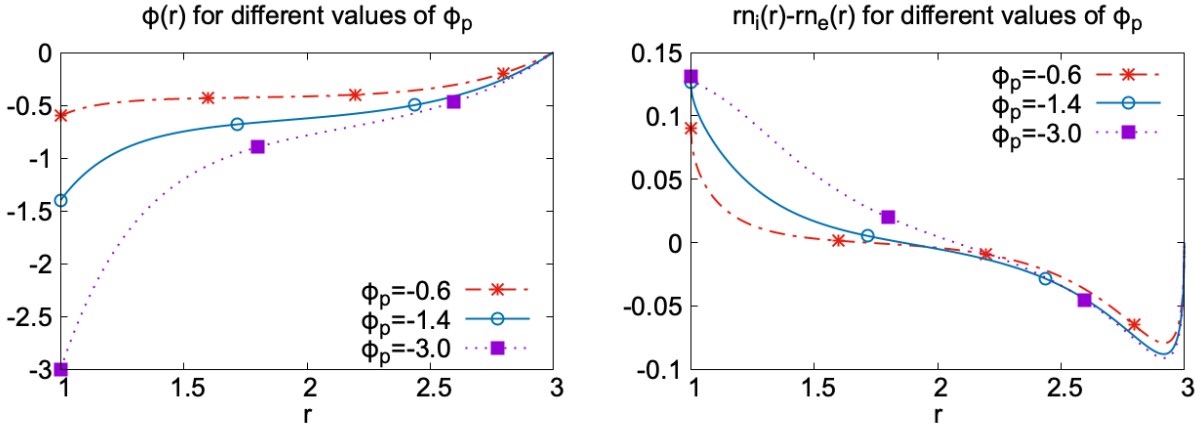


Figure 6: Radial case with unsatisfied Bohm condition: potential $\phi(r)$ (left) and density difference $rn_i(r) - rn_e(r)$ (right) for $\phi_p$ varying from $-0.6$ to $-3$.

### *6.1.3. The probe characteristic*

In the case of radial solutions, the total current at the probe is given by:

$$(j_i - j_e)(1) = \int_{-\infty}^{0} g_i^b(w)\, w\, dw - \frac{1}{\sqrt{\mu}} \int_{-\infty}^{-\sqrt{-2\phi_p}} g_e^b(w)\, w\, dw. \tag{108}$$

We see that it is a monotone increasing function of $\phi_p < 0$. Its value is independent of the Debye length $\lambda$ since $\phi_p$ is independent of $\lambda$. It moreover admits an asymptotic limit as $\phi_p \longrightarrow -\infty$ which is exactly

$$\lim_{\phi_p \to -\infty} (j_i - j_e)(1) = \int_{-\infty}^{0} g_i^b(w)\, w\, dw \ < 0. \tag{109}$$

It means that for very large (absolute) value of $\phi_p$ the collected current by the probe is essentially the ionic current. It is the expected behavior since the probe is repulsive for the

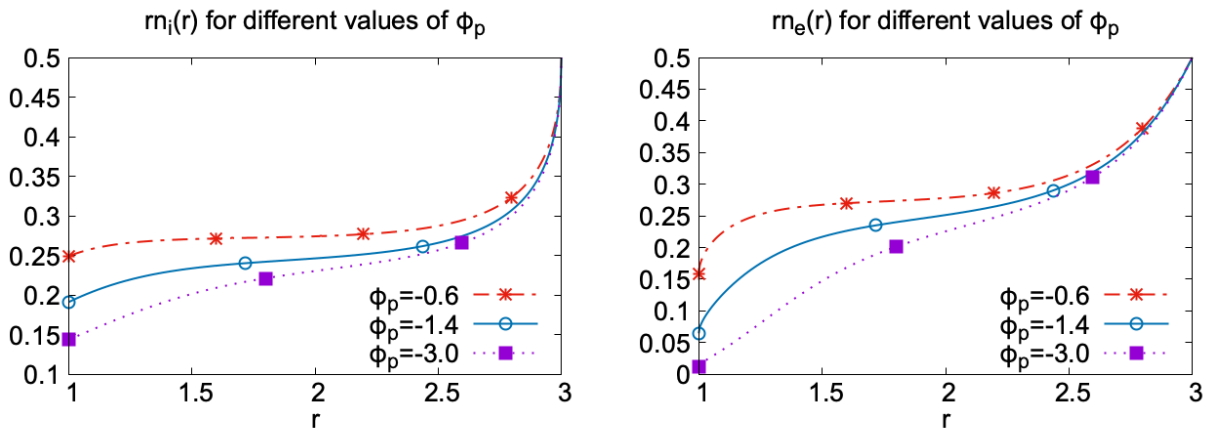


Figure 7: Radial case with unsatisfied Bohm condition: ionic density $rn_i(r)$ (left) and electronic density $rn_e(r)$ (right) for $\phi_p$ varying from $-0.6$ to $-3$.

electrons. It is also possible to prove [1] that there exists a unique value of $\phi_p < 0$ such that one has both $(j_i - j_e)(1) = 0$ and $n_i(r_b) = n_e(r_b)$. This value is known as the floating potential value. It is the case in practice when the probe is isolated from an exterior electrical circuit.

The total current in the case where the Bohm condition is satisfied (resp. unsatisfied) is plotted on Figure 8 left (resp. right). Parameters are the same as in the two previous subsections.

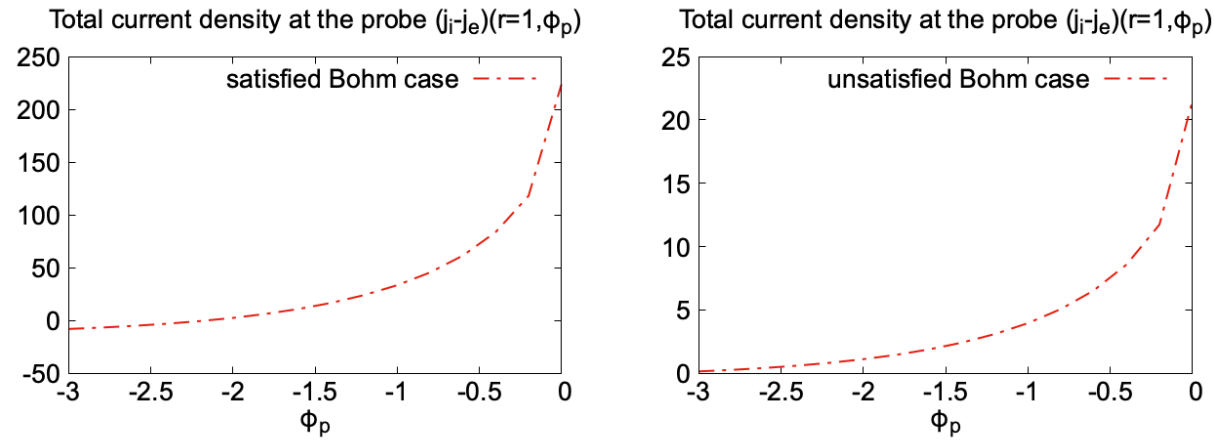


Figure 8: Radial case: total current density at the probe $(j_i - j_e)(r = 1, \phi_p)$ as a function of the probe potential, the Bohm condition being satisfied (left) or unsatisfied (right).

### *6.2. Non radial solutions*

We consider now the case of incoming distribution functions given by (103)-(104) with small values of $T > 0$. The incoming distributions functions in the radial velocity variable are the same as for the previous case of *radial solutions*, given by (105) and (107). We still

determine the positive constant $n^b > 0$ such that the core plasma is locally neutral that is $n_i(r_b) = n_e(r_b)$ but this time with the formula (17).

First, we are interested on macroscopic quantities when $\phi_p = -3$ for two values of the temperature: $T = 0.05$ and $T = 0.1$.

Figure 9 shows the potential $\phi(r)$, $r \in [1, r_b = 3]$ (on the left) and the difference $rn_i(r) - rn_e(r)$ (on the right), whereas Figure 10 represents the macroscopic densities $rn_i(r)$ (on the left) and $rn_e(r)$ (on the right). We notably observe that the function $rn_e$ is no longer monotone increasing: it has a strict local mimima in the interval $[1.5, 2]$. This can be explained due to the presence of trapped orbits which are unpopulated in the phase space of Figure 13.

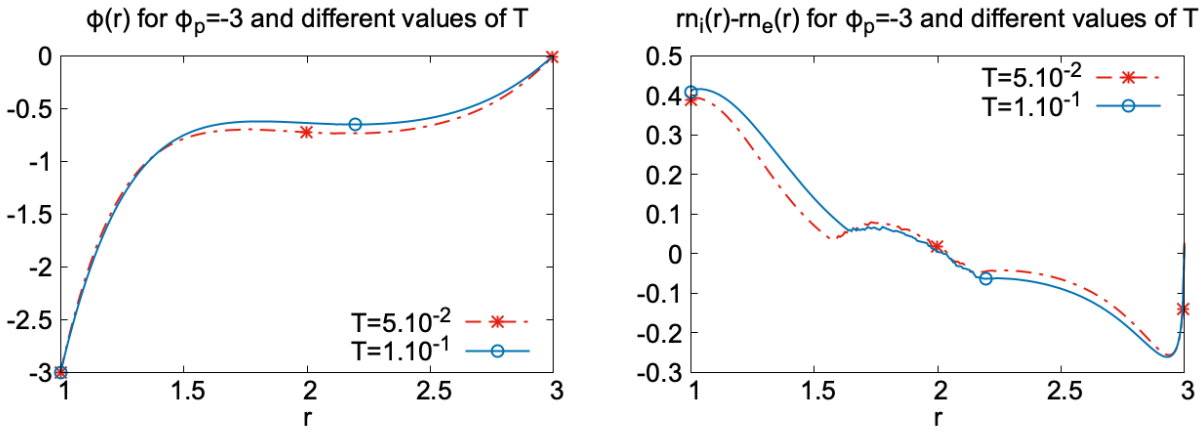


Figure 9: Perturbative case with unsatisfied Bohm condition: potential $\phi(r)$ (left) and density difference $rn_i(r) - rn_e(r)$ (right) for $\phi_p = -3$ and two values of T: 0.05 and 0.1.

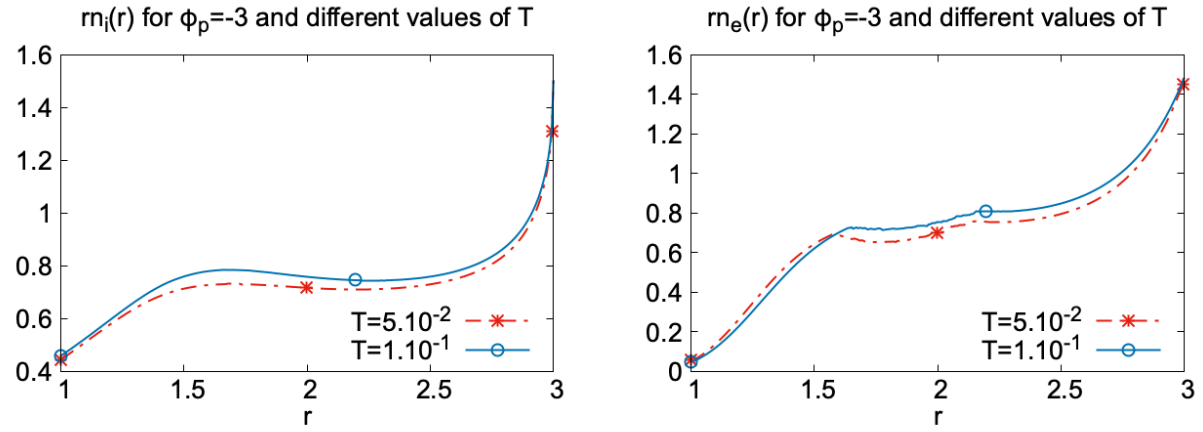


Figure 10: Perturbative case with unsatisfied Bohm condition: ionic density $rn_i(r)$ (left) and electronic density $rn_e(r)$ (right) for $\phi_p = -3$ and two values of T: 0.05 and 0.1.

Now, we discuss the phase space distribution functions. We first look, on Figure 12, at the ionic distribution $f_i(r, v_r)$ for three values of the angular velocity $v_\theta$ (increasing from top

to bottom) and for both values of temperature: $T = 0.05$ on the left and $T = 0.1$ on the right ($\phi_p$ is still fixed to -3). We see that when the temperature is equal to $T = 0.1$ and the angular velocity is $v_\theta = 0.91$ the phase space shows trajectories that comes from the core plasma with negative radial velocities, turn around the probe and goes back into the plasma with positive radial velocities.

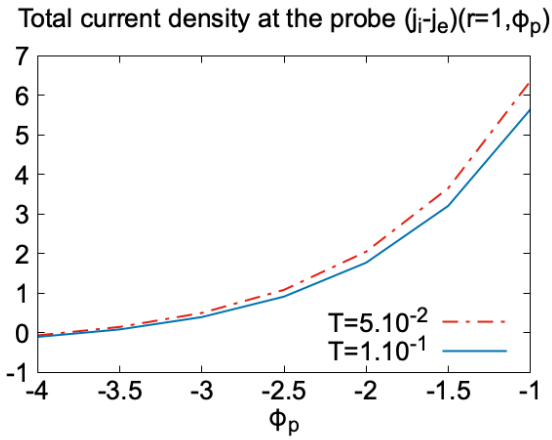


Figure 11: Perturbative case with unsatisfied Bohm condition: total current density at the probe $(j_i - j_e)(r = 1, \phi_p)$ as a function of the probe potential.

We represent for the same parameters the electronic distribution function $f_e(r, v_r)$ on Figure 13.

*6.2.1. Comments on the probe characteristic*

For both values of the temperature $T = 0.05$ and $T = 0.1$, we present the total current density at the probe $(j_i - j_e)(r = 1, \phi_p)$ as a function of $\phi_p$ in Figure 11. We still observe that it is monotone with respect to the probe potential value $\phi_p$ but it has not been proven. We also see that for each case, there is one unique value for which the current vanishes, it is the so called *floating potential* which corresponds to the case where the probe is isolated from any electrical circuit.

*6.2.2. Comments on particles trajectories*

We finally propose to represent some particles trajectories in the 2D space domain as drawn on Figure 1. Knowing, from our numerical method, the potential solution of the

stationary problem (1)-(2)-(3), we can solve ion and electron trajectories given by

$$\frac{dr}{dt}(t) = v_r(t) \tag{110}$$

$$\frac{dv_r}{dt}(t) = \frac{v_\theta^2(t)}{r(t)} \pm \partial_r \phi(r) \tag{111}$$

$$\frac{dv_\theta}{dt}(t) = -\frac{v_r(t)v_\theta(t)}{r(t)} \tag{112}$$

$$\frac{d\theta}{dt}(t) = \frac{v_\theta(t)}{r(t)} \tag{113}$$

where $\pm$ corresponds to a positive sign for electrons and to a negative one for ions. For a prospective study, we use a simple explicit scheme of order 1 in space and time given by finite differences approximations.

We consider the last case with $\phi_p = -3$ and $T = 0.1$, for which the potential solution $\phi$ has been determined as explained in the beginning of this subsection. In Figure 14 we represent the trajectories in plan $(x, y) = (r\cos(\theta), r\sin(\theta))$ of an electron for 4 different velocity initializations $(v_r(t = 0), v_\theta(t = 0))$. At $t = 0$, the particle enters the system at position $(r(t = 0) = r_b = 3, \theta(t = 0) = \frac{\pi}{4})$. Final time corresponds to either an exit of the system, or a contact with the probe. The coloured background are iso values of $\phi$, solution of the stationary problem. On the top left plot, angular velocity $v_\theta(0) = 0.5$ is small whereas radial velocity $|v_r(0)| = 3$ is high, so that electron is not deviated by $\phi$ and reaches the probe. On the bottom left plot, radial velocity $|v_r(0)| = 2$ is smaller so that electron is deviated by $\phi$ without reaching the probe, and then it goes out of the system. This phenomena is amplified on the top right plot where $|v_r(0)| = 1$. Finally, with high values of angular $v_\theta(0) = 2$ and radial $|v_r(0)| = 3$ velocities, $\phi$ has no big influence on the trajectory of the electron.

We represent on Figure 6.2.2 ion trajectories. On the top left plot, angular velocity $v_\theta(0) = 0.5$ is small and radial velocity $|v_r(0)| = 1$ is high enough to go quite directly on the probe. A second configuration is plotted on the top right: $v_\theta(0) = 1$, $|v_r(0)| = 0$ and ion stays quite far from the probe. On the bottom left plot, $v_\theta(0) = 0.75$, $|v_r(0)| = 0.5$ and the particle finishes to be attracted by the probe, whereas on the bottom right plot, $v_\theta(0) = 0.79$, $|v_r(0)| = 0.65$ is a configuration where the particle is able to bypass the probe.

## References


[1] M. Badsi, M. Campos Pinto, and B. Després. A minimization formulation of a bi-kinetic sheath. *Kinetic and related models*, 9(4), 2016.

[2] M. Badsi and L. Godard-Cadillac. Existence of solutions for a bi-species kinetic model of a cylindrical langmuir probe. *to appear in Communication in Mathematical Sciences*, 2022. preprint, `arXiv:2201.02681`.

[3] D. Bohm. The characteristics of electrical discharges in magnetic fields. *New York: Mc Graw Hill*, 1949.

[4] Francis F. Chen. *Introduction to Plasma Physics and controlled fusion*. Springer, 1984.

[5] D. Darian, S.Marholm, M. Mortensen, and W.J. Miloch. *Theory and simulations of spherical and cylindrical Langmuir probes in non-Maxwellian plasmas*, volume 61. Plasma Physics and controlled fusion, 2019.

[6] P. Degond, S. Jaffard, F. Poupaud, and P. A. Raviart. The child-langmuir asymptotics of the vlasov-poisson equation for cylindrically or spherically symmetric diodes. part 1: Statement of the problem and basic estimates. *Math. Meth. Appl. Sci.*, 19:287–312, 1996.

[7] P. Degond, S. Jaffard, F. Poupaud, and P. A. Raviart. The child-langmuir asymptotics of the vlasov-poisson equation for cylindrically or spherically symmetric diodes. part 2: Analysis of the reduced problem and determination of the child-langmuir current. *Math. Meth. Appl. Sci.*, 19:313–340, 1996.

[8] D. Gérard-Varet, D. Han-Kwan, and F. Rousset. Quasineutral limit of the euler-poisson system for ions in a domain with boundaries. *Indiana Univ. Math. J. 62*, pages 359–402, 2013.

[9] R. Glowinski. *Numerical methods for nonlinear variational problems*. Springer-Verlag, 1984.

[10] J.G Lamframboise. Theory of spherical and cylindrical langmuir probes in a collisionless Maxwellian plasma at rest. *Institute for Aerospace studies, University of Toronto*, 1966.

[11] H Mott-Smith and I Langmuir. *Physical review*, 28, 1926.

[12] F.W. Olver, D.W Lozier, R.F Boisvert, and C.W Clark. *NIST Handbook of mathematical functions*. Cambridge University Press, 2010.

[13] P.A Raviart and C. Greengard. A boundary-value problem for the stationary vlasov-poisson equations: the plane diode. *Communications on Pure and Applied Mathematics*, 1990.

[14] K.U Riemann. The Bohm criterion and sheath formation. *Physics of Plasmas*, 1991.

[15] G. Sanchez-Arriaga. *A direct Vlasov code to study the non-stationary current collection by a cylindrical Langmuir probe*, volume 20. Physics of Plasmas, 2013.

[16] G. Sanchez-Arriaga and D. Pastor-Moreno. *Direct Vlasov simulations of electron-attracting cylindrical Langmuir probes in flowing plasmas*. Physics of Plasmas, 2014.

[17] G. Stampachia and D. Kinderlehrer. *An introduction to variational inequalities and their applications*. Academic Press, 1980.

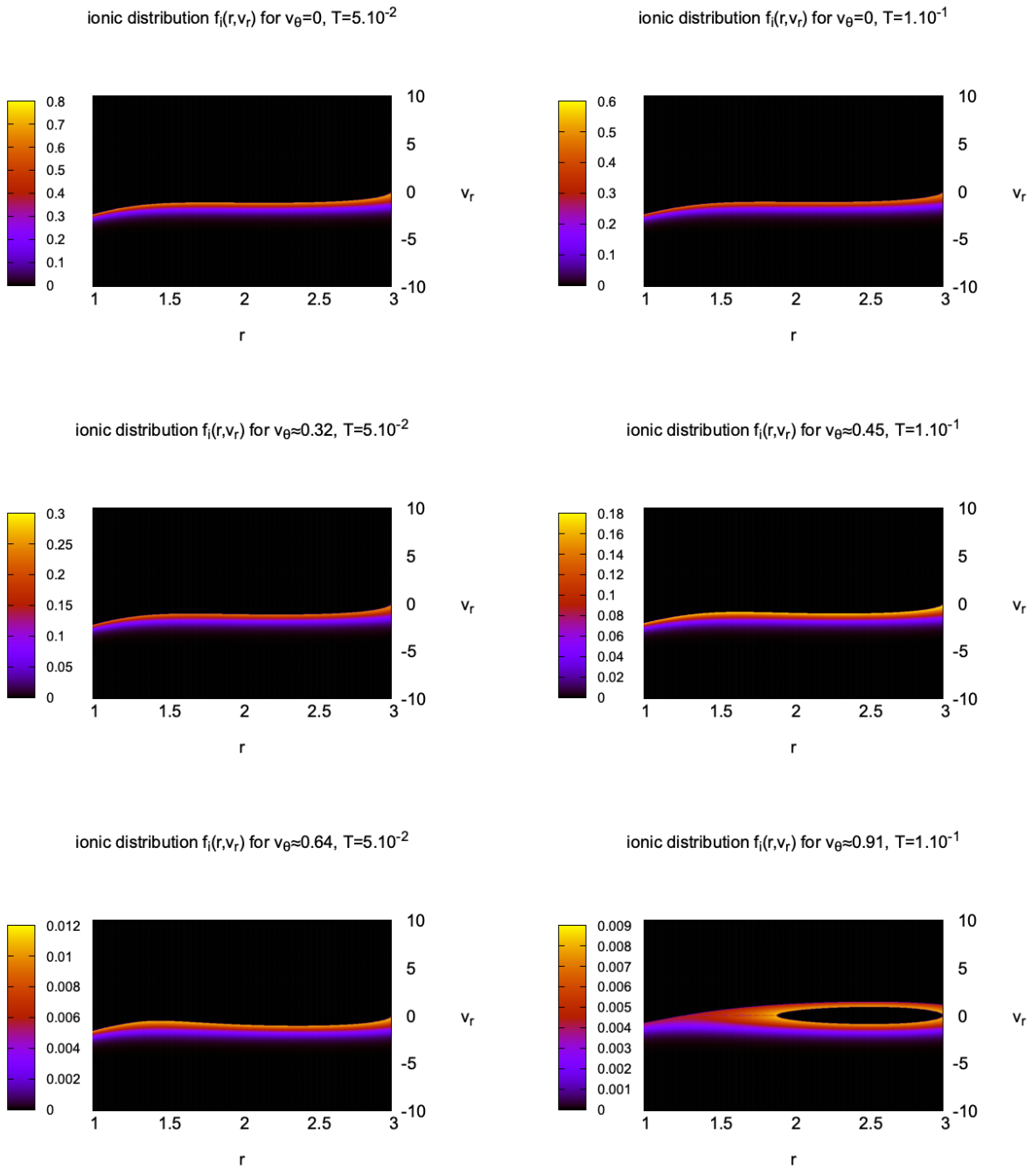


Figure 12: Perturbative case with unsatisfied Bohm condition: ionic distribution function $f_i(r, v_r)$ for $T = 0.05$ (left), $T = 0.1$ (right), and three increasing values of $v_\theta$ from top to bottom.

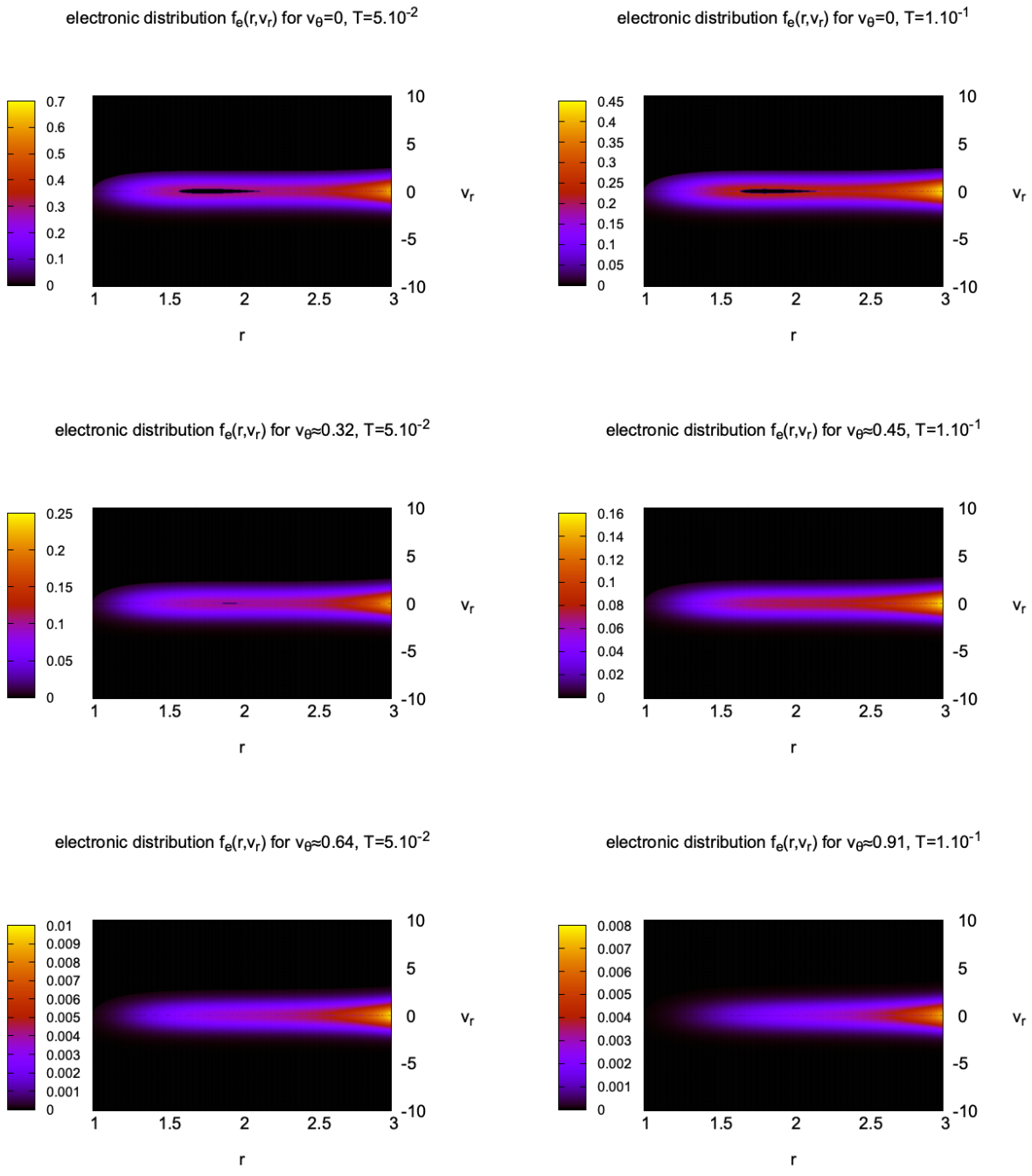


Figure 13: Perturbative case with unsatisfied Bohm condition: ionic distribution function $f_e(r, v_r)$ for $T = 0.05$ (left), $T = 0.1$ (right), and three increasing values of $v_\theta$ from top to bottom.

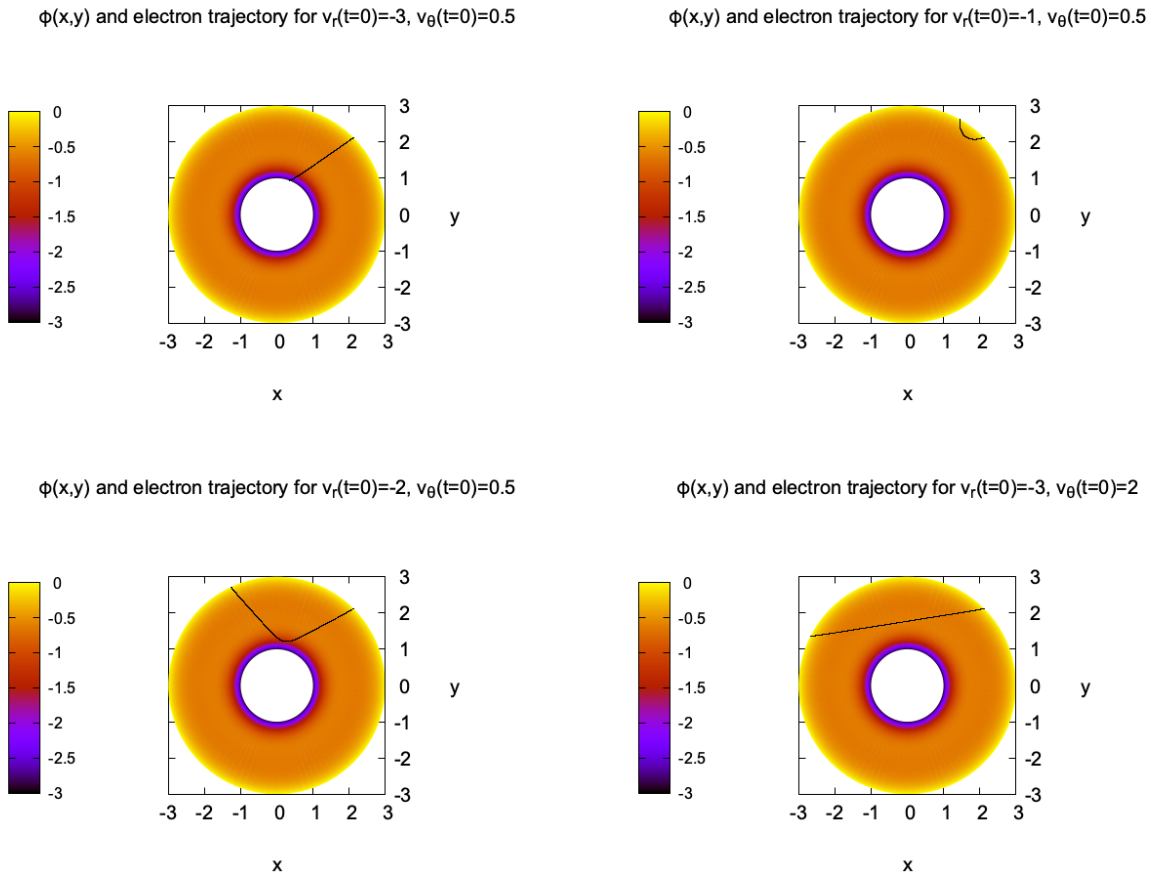


Figure 14: Perturbative case with unsatisfied Bohm condition: *phi* and trajectories of electrons.

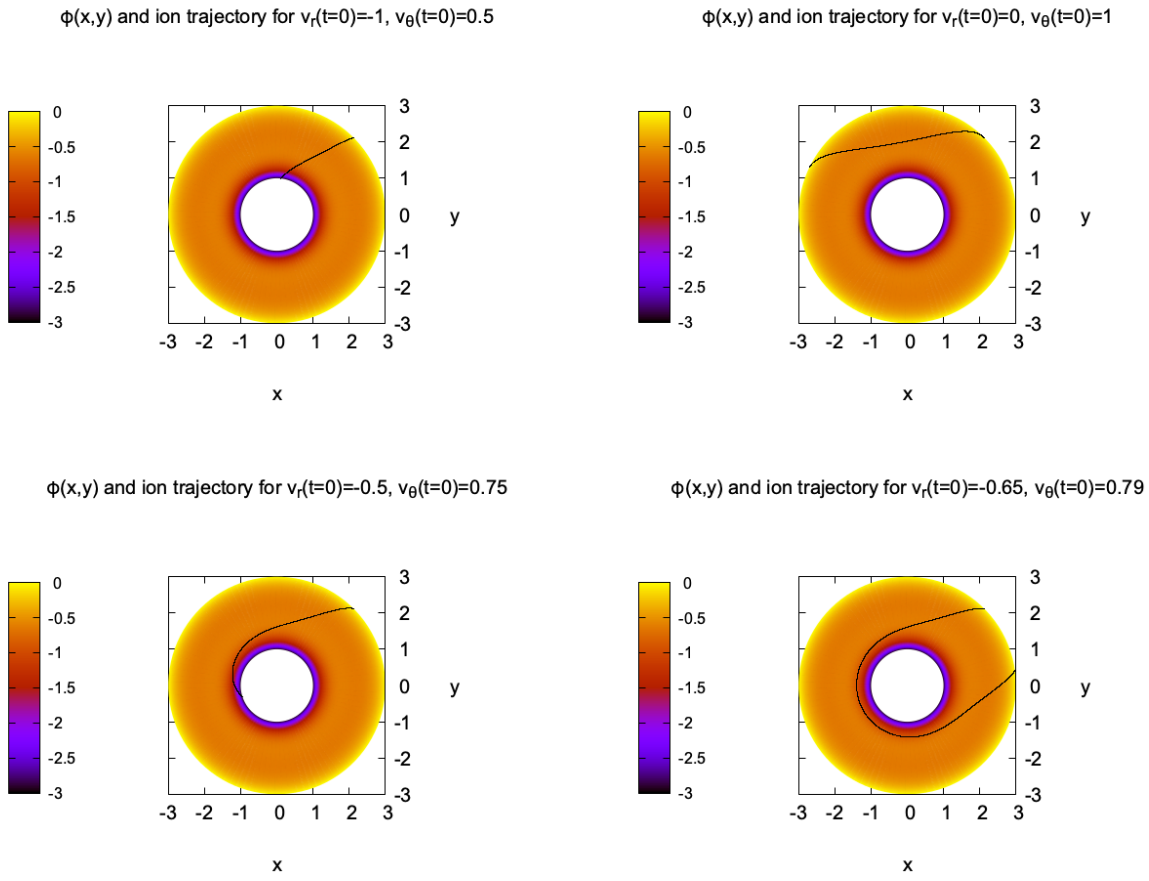


Figure 15: Perturbative case with unsatisfied Bohm condition: *phi* and trajectories of ions.